De novo variants in *FRYL* are associated with developmental delay, intellectual disability, and dysmorphic features

Authors

Xueyang Pan, Alice M. Tao, Shenzhao Lu, ..., Shinya Yamamoto, Wendy K. Chung, Hugo J. Bellen

Correspondence

wendy.chung@childrens.harvard.edu (W.K.C.), hbellen@bcm.edu (H.J.B.)

We report fourteen individuals with *de novo* variants in *FRYL* who present with neurodevelopmental features. Nine variants correspond to premature stop codons, frameshifts, or splicing variants. Modeling in *Drosophila* supports an essential developmental function for the fly *FRYL* ortholog; genomic integration of three missense variants caused a loss-of-function phenotype.

Pan et al., 2024, The American Journal of Human Genetics *111*, 1–19
April 4, 2024

https://doi.org/10.1016/j.ajhg.2024.02.007

Please cite this article in press as: Pan et al., *De novo* variants in *FRYL* are associated with developmental delay, intellectual disability, and dysmorphic features, The American Journal of Human Genetics (2024), https://doi.org/10.1016/j.ajhg.2024.02.007

ARTICLE

De novo variants in *FRYL* are associated with developmental delay, intellectual disability, and dysmorphic features

Xueyang Pan,[1,2] Alice M. Tao,[3] Shenzhao Lu,[1,2] Mengqi Ma,[1,2] Shabab B. Hannan,[1,2] Rachel Slaugh,[4] Sarah Drewes Williams,[5] Lauren O'Grady,[6,7] Oguz Kanca,[1,2] Richard Person,[8] Melissa T. Carter,[9] Konrad Platzer,[10] Franziska Schnabel,[10] Rami Abou Jamra,[10] Amy E. Roberts,[11,12] Jane W. Newburger,[11,13] Anya Revah-Politi,[14] Jorge L. Granadillo,[4] Alexander P.A. Stegmann,[15] Margje Sinnema,[15] Andrea Accogli,[16,17] Vincenzo Salpietro,[18] Valeria Capra,[19] Lina Ghaloul-Gonzalez,[5,20] Martina Brueckner,[21,22] Marleen E.H. Simon,[23] David A. Sweetser,[6,24] Kevin E. Glinton,[1,25] Susan E. Kirk,[26,27] Baylor College of Medicine Center for Precision Medicine Models, Michael F. Wangler,[1,2] Shinya Yamamoto,[1,2,28] Wendy K. Chung,[29,*] and Hugo J. Bellen[1,28,*]

Summary

FRY-like transcription coactivator (FRYL) belongs to a Furry protein family that is evolutionarily conserved from yeast to humans. The functions of FRYL in mammals are largely unknown, and variants in *FRYL* have not previously been associated with a Mendelian disease. Here, we report fourteen individuals with heterozygous variants in *FRYL* who present with developmental delay, intellectual disability, dysmorphic features, and other congenital anomalies in multiple systems. The variants are confirmed *de novo* in all individuals except one. Human genetic data suggest that *FRYL* is intolerant to loss of function (LoF). We find that the fly *FRYL* ortholog, *furry* (*fry*), is expressed in multiple tissues, including the central nervous system where it is present in neurons but not in glia. Homozygous *fry* LoF mutation is lethal at various developmental stages, and loss of *fry* in mutant clones causes defects in wings and compound eyes. We next modeled four out of the five missense variants found in affected individuals using *fry* knockin alleles. One variant behaves as a severe LoF variant, whereas two others behave as partial LoF variants. One variant does not cause any observable defect in flies, and the corresponding human variant is not confirmed to be *de novo*, suggesting that this is a variant of uncertain significance. In summary, our findings support that *fry* is required for proper development in flies and that the LoF variants in *FRYL* cause a dominant disorder with developmental and neurological symptoms due to haploinsufficiency.

Introduction

FRYL (FRY-like transcription coactivator, also known as AF4p12) belongs to an evolutionarily conserved protein family, which is named after the fruit fly Furry (Fry) protein,[1] the first member identified in the family. Furry proteins are large proteins (FRYL has 3,013 amino acid residues) with a number of conserved regions (Figure 1A), including a FRY N-terminal domain (FND) predicted to fold into a large number of HEAT/Armadillo repeats[2] and a C-terminal region predicted to have two leucine zipper motifs and a coiled-coil motif (only present in vertebrate orthologs).[3] The other conserved regions do not show similarity to any well-characterized motif.[2] In model organisms, Furry family proteins have diverse functions, including cell polarity maintenance,[4,5] cell morphogenesis,[1,6] arborization and tiling of dendrites,[2,7,8] and transcriptional regulation.[3]

Humans have two Furry paralogs, FRY and FRYL, which share 61% identity and 75% similarity. In mammalian

[1]Department of Molecular and Human Genetics, Baylor College of Medicine, Houston, TX, USA; [2]Jan & Dan Duncan Neurological Research Institute, Texas Children's Hospital, Houston, TX, USA; [3]Vagelos School of Physicians and Surgeons, Columbia University, New York, NY, USA; [4]Division of Genetics and Genomic Medicine, Department of Pediatrics, Washington University in St. Louis School of Medicine, St. Louis, Missouri, USA; [5]Division of Genetic and Genomic Medicine, Department of Pediatrics, UPMC Children's Hospital of Pittsburgh, Pittsburgh, PA, USA; [6]Division of Medical Genetics & Metabolism, Massachusetts General for Children, Boston, MA, USA; [7]MGH Institute of Health Professions, Charlestown, MA, USA; [8]GeneDx, LLC, Gaithersburg, MD, USA; [9]Department of Genetics, Children's Hospital of Eastern Ontario, Ottawa, ON, Canada; [10]Institute of Human Genetics, University of Leipzig Medical Center, Leipzig, Germany; [11]Department of Cardiology, Boston Children's Hospital, Boston, MA, USA; [12]Department of Medicine, Division of Genetics, Boston Children's Hospital, Boston, MA, USA; [13]Department of Pediatrics, Harvard Medical School, Boston, MA, USA; [14]Institute for Genomic Medicine and Precision Genomics Laboratory, Columbia University Irving Medical Center, New York, NY, USA; [15]Department of Clinical Genetics, Maastricht University Medical Center, Maastricht, the Netherlands; [16]Division of Medical Genetics, Department of Medicine, McGill University Health Center, Montreal, QC, Canada; [17]Department of Human Genetics, McGill University, Montreal, QC, Canada; [18]Department of Neuromuscular Disorders, University College London Institute of Neurology, Queen Square, London, UK; [19]Unit of Medical Genetics and Genomics, IRCCS Istituto Giannina Gaslini, Genoa, Italy; [20]Department of Human Genetics, Graduate School of Public Health, University of Pittsburgh, Pittsburgh, PA, USA; [21]Department of Pediatrics, Yale University School of Medicine, New Haven, CT, USA; [22]Department of Genetics, Yale University School of Medicine, New Haven, CT, USA; [23]Department of Medical Genetics, University Medical Center Utrecht, Utrecht, the Netherlands; [24]Center for Genomic Medicine, Massachusetts General Hospital, Boston, MA, USA; [25]Department of Genetics, Texas Children's Hospital, Houston, TX, USA; [26]Section of Hematology/Oncology, Department of Pediatrics, Baylor College of Medicine, Houston, TX, USA; [27]Texas Children's Cancer and Hematology Center, Houston, TX, USA; [28]Department of Neuroscience, Baylor College of Medicine, Houston, TX, USA; [29]Departments of Pediatrics, Boston Children's Hospital, Harvard Medical School, Boston, MA, USA
*Correspondence: wendy.chung@childrens.harvard.edu (W.K.C.), hbellen@bcm.edu (H.J.B.)
https://doi.org/10.1016/j.ajhg.2024.02.007.

Please cite this article in press as: Pan et al., *De novo* variants in *FRYL* are associated with developmental delay, intellectual disability, and dysmorphic features, The American Journal of Human Genetics (2024), https://doi.org/10.1016/j.ajhg.2024.02.007

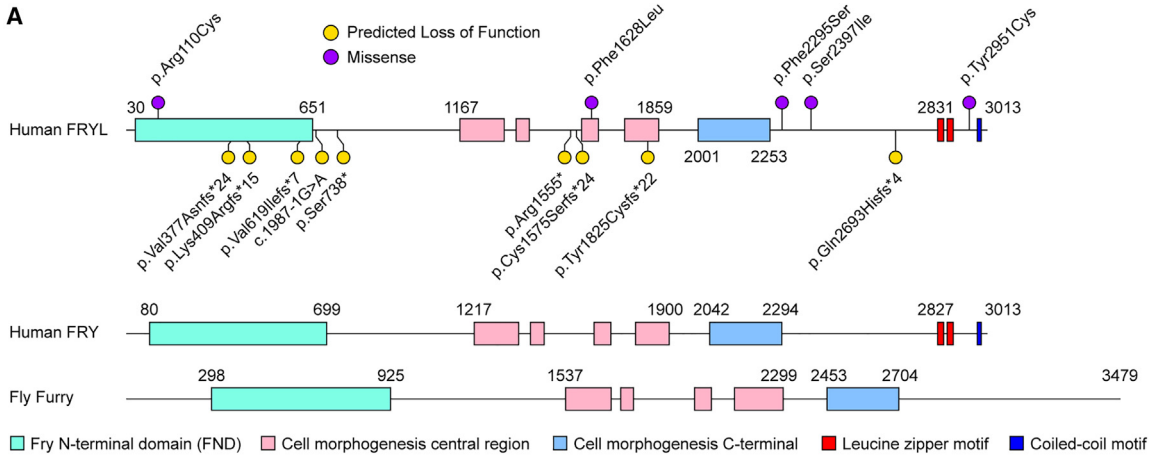

B

Amino Acid Location	110	1628	2295	2397	2951
H. sapiens (human) FRYL - reference	R	F	F	S	Y
H. sapiens (human) FRY	R	F	F	S	Y
M. mulatta (rhesus) FRYL	R	F	F	S	Y
M. musculus (mouse) Fryl	R	F	F	S	Y
C. lupus familiaris (dog) FRYL	R	F	F	S	Y
L. africana (elephant) FRYL	R	F	F	S	Y
G. gallus (chicken) FRYL	R	F	F	S	Y
X. tropicalis (frog) Fryl	R	F	F	S	Y
D. rerio (zebrafish) Fryl	R	F	F	S	Y
D. melanogaster (fruit fly) Fry	V	F	F	S	Y
C. elegans (roundworm) SAX-2	--	I	F	S	F
S. cerevisiae (budding yeast) Tao3p	K	I	--	G	--
S. pombe (fission yeast) Mor2p	--	F	--	T	--
FRYL missense variant - affected individuals	C	L	S	I	C

Figure 1. Locations of predicted LoF and missense FRYL variants identified in this study

(A) Schematic of human FRYL and its alignment to human FRY and fly Fry. The Fry N-terminal (Pfam: #14222), cell morphogenesis central (Pfam: #PF14225), and cell morphogenesis C-terminal domains (Pfam: #PF14228) are identified in the Pfam project.[9] The C-terminal leucine zipper and coiled-coil motifs are predicted by Goto et al.,[3] which are only present in human FRY and FRYL but not fly Fry. Five FRYL missense variants identified in this study are shown above the protein, and nine predicted LoF variants are shown below the protein.

(B) The conservation of the five amino acid residues affected by the *FRYL* missense variants. The "–" symbols indicate that no aligned amino acid residue is found in the corresponding protein. All the residues are conserved in the Fryl proteins across vertebrate species as well as human FRY. In *Drosophila*, which is used as model organism in this study, four residues are conserved while the Arg110 residue is not. The variants identified in the five affected individuals correspond to amino acid changes, which are shown on the bottom row.

cells, FRY has been shown to regulate microtubule bundling and spindle organization during mitosis.[10–12] Variants in *FRY* (MIM: 614818) are associated with cancer susceptibility and progression in patient-derived cancer cell lines and carcinogen-induced mammalian cancer models.[13,14] In humans, homozygous variants in *FRY* have been observed in individuals with intellectual disability in three consanguineous families.[15–17] However, due to the insufficient number of affected individuals and the consanguineous nature of the families, the association between *FRY* variants and the intellectual disability phenotype has not been robustly established. *FRYL* was first identified in a *FRYL*-mixed lineage leukemia (*MLL*) fusion gene in an individual with lymphoblastic leukemia.[18] Full-length FRYL was later found to interact with the active intracellular domain of NOTCH1 (ICN1).[19] ICN1 translocates into the nucleus and functions with other coactivators to activate transcription of target genes;[20] however, how FRYL regulates this process is unknown. Most *Fryl* homozygous mutant mice die shortly after birth, and rare escapers survive less than a year and present with growth retardation and defects in kidney development.[21] Morpholino-mediated knockdown of *fryl* in zebrafish causes cardiac and craniofacial defects during development.[22] One individual with a heterozygous *de novo* variant in *FRYL* was identified in the Deciphering Developmental Disorders (DDD) study who presented with short stature and craniofacial and cardiac defects.[22]

Here, we report thirteen individuals who have *de novo* heterozygous variants in *FRYL* and one individual with heterozygous *FRYL* variant that is not confirmed to be *de novo*. The individuals present with developmental delay (DD), intellectual disability, dysmorphic features, and other congenital anomalies in cardiovascular, skeletal, gastrointestinal,

Please cite this article in press as: Pan et al., *De novo* variants in *FRYL* are associated with developmental delay, intellectual disability, and dysmorphic features, The American Journal of Human Genetics (2024), https://doi.org/10.1016/j.ajhg.2024.02.007

Figure 2. Dysmorphic facial features of individuals with heterozygous variants in *FRYL*

(A and B) Facial images of individual 1 showing bitemporal narrowing, tall forehead, hypertelorism, epicanthal folds, upslanting palpebral fissures, flat nasal bridge with short upturned nose with bulbous tip, long deeply grooved philtrum, and cleft chin.

(C and D) Facial images of individual 6 showing hypertelorism, epicanthal folds, flat nasal bridge, and ear pit (indicated by the arrow).

renal, and urogenital systems. Using fruit flies, we find that the fly *FRYL* ortholog *furry* (*fry*) is required for fly development, consistent with previous reports.[1,6] Using *fry* knockin alleles analogous to human missense variants, we provide evidence that three out of the five missense variants found in affected individuals cause an LoF. These data support that haploinsufficiency in *FRYL* likely underlies a disorder with developmental and neurological symptoms.

Material and methods

Recruitment and sequencing of individuals

The cohort of individuals described in this study was recruited through the Pediatric Cardiac Genomics Consortium (individuals 3 and 9), the SPARK consortium (individual 12), and matchmaking via GeneMatcher (11 individuals).[23] Clinical data were obtained after written informed consent was provided by a parent or legal guardian at the institution at which they were enrolled for all individuals. The study of the individuals was approved by the Columbia University Institutional Review Board. The clinical data were supplied by the clinicians at each of the centers and then reviewed centrally by two clinicians who harmonized the data across the cases in collaboration with the clinicians at each site. The clinical features of the individuals and their variants in *FRYL* are summarized in Figures 1 and 2 and Tables 1 and 2.

Whole-exome sequencing of all but one family (individual 6) was performed to detect genetic variants. Individual 6 was tested by exome sequencing targeting gene panels for intellectual disabilities, multiple congenital anomalies (MCA), and congenital heart disease (CHD). Trio sequencing was included in the analysis to identify *de novo* variants, except one family (individual 13) for whom only paternal exome sequencing was completed due to lack of availability of the mother. The gnomAD database was used to assess variant frequency in the general population.[26] *In silico* algorithms, including PolyPhen-2,[27] MutationTaster,[28] SIFT,[29] PROVEAN,[30,31] CADD,[32] REVEL,[33] and M-CAP,[34] were employed to predict the pathogenicity of the variants. The American College of Medical Genetics and Genomics (ACMG) and the Association for Molecular Pathology (AMP) guideline for variant interpretation was also employed to evaluate the pathogenicity of the variants.[35]

Drosophila stocks and maintenance

Flies were cultured using standard fly food at 25°C on a 12-h light/dark cycle. The *fry* knockin lines and fry^{GFP} line were generated in house for this study (see methods below). The *ubxFLP; ; ubi-GFP FRT80B* and *vas-phiC31; ; VK33* lines were from the Bellen lab stock. All other fly lines were obtained from the Bloomington Drosophila Stock Center (BDSC) (see Table S1).

Generation of the fry^{GFP} allele

The fry^{GFP} allele was generated by a well-established recombination-mediated cassette exchange (RMCE)-based strategy (Figure S1).[36] Females carrying *hs-flippase* (*FLP*), *vas-phiC31*, and *flippase recognition target* (*FRT*)*-attB-EGFP-FlAsH-StrepII-TEVcs-3xFlag* (*GFSTF*)*-attB-white*$^{+}$*-FRT* cassette with correct phase (phase I) were crossed to $fry^{MI12326}$ males. Upon heat shock, the FRT-flanked cassette was flipped out as a circular DNA in the presence of Flippase, and the GFSTF sequence was swapped into the $fry^{MI12326}$ Minos-mediated integration cassette (MiMIC) site by phiC31-mediated RMCE. The progenies with fry^{GFP} allele were selected by the loss of *white* and *yellow* markers. The resulting fry^{GFP} allele was verified by PCR using the GFSTF_ver_L and GFSTF_ver_R primers listed in Table S2. The publicly available fly lines used in this protocol are listed in Table S1.

Generation of *fry* knockin lines by prime editing

Two knockin alleles, $fry^{p.Phe2024Leu}$ and $fry^{p.Phe2746Ser}$, were generated by prime editing following a published protocol with adaptations.[37]

Please cite this article in press as: Pan et al., *De novo* variants in *FRYL* are associated with developmental delay, intellectual disability, and dysmorphic features, The American Journal of Human Genetics (2024), https://doi.org/10.1016/j.ajhg.2024.02.007

Table 1. Predicted LoF and deleterious missense variants in *FRYL*

	Variant		Inheritance	Method used to detect variant	Chr 4 coordinates (hg19/hg38)	gnomAD frequency	ACMG classification	Polyphen-2	Mutation taster	SIFT	PROVEAN	CADD	REVEL	M-CAP
Predicted LoF														
Individual 1	c.1129_1130delGT	p.Val377Asnfs*24	*de novo*	whole-exome sequencing	48597923 48595905	–	likely pathogenic (PVS1, PS2, PM2)	N/A	D	N/A	N/A	N/A	N/A	N/A
Individual 2	c.1224del	p.Lys409Argfs*15	*de novo*	whole-exome sequencing	48597631 48595613	–	likely pathogenic (PVS1, PS2, PM2)	N/A	D	N/A	N/A	N/A	N/A	N/A
Individual 3	c.1855_1858del	p.Val619Ilefs*7	*de novo*	whole-exome sequencing	48584642 48582624	–	likely pathogenic (PVS1, PS2, PM2)	N/A	D	N/A	N/A	33	N/A	N/A
Individual 4	c.1987-1G>A	splice site acceptor variant	*de novo*	whole-exome sequencing	48583623 48581606	–	likely pathogenic (PVS1, PS2, PM2)	N/A	N/A	N/A	N/A	34	N/A	N/A
Individual 5	c.2210_2211dupTA	p.Ser738*	*de novo*	whole-exome sequencing	48582930 48580913	–	likely pathogenic (PVS1, PS2, PM2)	N/A	D	N/A	N/A	N/A	N/A	N/A
Individual 6	c.4663C>T	p.Arg1555*	*de novo*	exome sequencing gene panels for intellectual disabilities, MCAs, and CHD	48551611 48549594	–	likely pathogenic (PVS1, PS2, PM2)	D	D	D	N/A	40	N/A	N/A
Individual 7	c.4724del	p.Cys1575Serfs*24	*de novo*	whole-exome sequencing	48551550 48549532	–	likely pathogenic (PVS1, PS2, PM2)	N/A	D	N/A	N/A	N/A	N/A	N/A
Individual 8	c.5474_5475delAT	p.Tyr1825Cysfs*22	*de novo*	whole-exome sequencing	48545941 48543923	–	likely pathogenic (PVS1, PS2, PM2)	N/A	D	N/A	N/A	N/A	N/A	N/A
Individual 9	c.8079_8080del	p.Gln2693Hisfs*4	*de novo*	whole-exome sequencing	48514563 48512545	–	likely pathogenic (PVS1, PS2, PM2)	N/A	D	N/A	N/A	34	N/A	N/A
Missense														
Individual 10	c.328C>T	p.Arg110Cys	*de novo*	whole-exome sequencing	48621374 48619357	–	likely pathogeni (PVS1, PS2, PM2)	D	D	D	N	32	0.405	0.024
Individual 11	c.4882T>C	p.Phe1628Leu	*de novo*	whole-exome sequencing	48550713 48548696	–	likely pathogenic (PVS1, PS2, PM2)	D	D	D	D	28.5	0.589	0.015
Individual 12	c.6884T>C	p.Phe2295Ser	*de novo*	whole-exome sequencing	48533192 48531175	–	likely pathogenic (PVS1, PS2, PM2)	D	D	D	D	29.8	0.768	0.19
Individual 13	c.7190G>T	p.Ser2397Ile	not paternal (mother never tested)	whole-exome sequencing	48529621 48527604	4.02×10^{-6}	VUS (PP3)	D	D	D	D	25.5	0.428	0.095
Individual 14	c.8852A>G	p.Tyr2951Cys	*de novo*	whole-exome sequencing	48501629 48499612	–	likely pathogenic (PVS1, PS2, PM2)	D	D	D	D	27.4	0.639	0.096

CHD, congenital heart disease; D, deleterious; MCA, multiple congenital anomalies; N, neutral; N/A, not available; VUS, variant of uncertain significance.

Table 2. Detailed clinical findings of patients with heterozygous predicted LoF and missense *FRYL* variants

	Individual 1	Individual 2	Individual 3	Individual 4	Individual 5	Individual 6	Individual 7	Individual 8	Individual 9	Individual 10	Individual 11	Individual 12	Individual 13	Individual 14	Summary
Variant class	predicted LoF	predicted LoF	predicted LoF	predicted LoF	predicted LoF	predicted LoF	predicted LoF	predicted LoF	predicted LoF	missense	missense	missense	missense	missense	9 LoF (64%), 5 missense (36%)
Variant in *FRYL*	p.Val377Asnfs*24	p.Lys409Argfs*15	p.Val619Ilefs*7	c.1987-1G>A	p.Ser738*	p.Arg1555*	p.Cys1575Serfs*24	p.Tyr1825Cysfs*22	p.Gln2693Hisfs*4	p.Arg110Cys	p.Phe1628Leu	p.Phe2295Ser	p.Ser2397Ile	p.Tyr2951Cys	–
Sex	F	F	M	M	M	M	F	M	M	M	M	M	F	M	4 F (28%), 10 M (72%)
Current age (years)	3.25	19	10	deceased (0.3)	12	2.2	6	20	8.8	15	12	8	21	9	average: 11.3
Prenatal complications	none	premature placental abruption	none	none	pre-eclampsia, HELLP syndrome, premature delivery (26 weeks)	short long bones	none	none	umbilical cord around neck at birth, forceps-assisted delivery, and torticollis	increased nuchal translucency	none	none	premature delivery (33 weeks)	C-section due to maternal hypertension and failure to progress, maternal diabetes	–
Birth weight (kg) (*Z* score)	2.14 (−1.65)	3.35 (-0.30)	3.35 (+0.53)	3.19 (+0.12)	0.62 (−1.35)	2.2 (−2.98)	2.88 (−0.73)	2.89 (−0.70)	2.1 (−3.37)	3.8 (+1.58)	3.89 (+1.12)	NR	NR	2.84 (−0.85)	2/14 (14%) with *Z* score < −2 average: −0.72
Birth length (cm) (*Z* score)	44 (−1.65)	49 (−1.23)	NR	51.5 (+0.9)	30.5 (−1.43)	NR	47 (−1.5)	NR	41 (−4.7)	NR	NR	NR	NR	47 (−1.5)	1/14 (7%) with *Z* score < −2 average: −1.59
Birth OFC (cm) (*Z* score)	31.5 (−1.65)	36.5 (1.23)	NR	35.5 (+1.5)	NR	NR	33.5 (+0.24)	NR	30.5 (−1.79)	NR	NR	NR	NR	33 (−0.08)	0/14 (0%) with *Z* score < −2 average: −0.09
Current weight (kg) (*Z* score)	10.9 (−4.00)	38.5 (−3.52)	20 (−0.30)	N/A	61.5 (+1.76)	9.7 (−2.0)	11.9 (-3.7)	90.2 (+1.32)	34.6 (+1.46)	56.9 (+2.4)	36.3 (−0.70)	NR	75.2 (+1.09)	37 (+1.12)	4/13 (31%) with *Z* score < −2 average: −0.42
Current length (cm) (*Z* score)	87 (−1.88)	159.6 (−1.33)	109.2 (−1.21)	N/A	147 (−0.28)	79 (−1.4)	98 (−3.6)	169.7 (-0.96)	131 (+0.09)	155.2 (-0.9)	146.1 (−0.42)	NR	155.5 (−1.19)	130 (−0.58)	1/13 (8%) with *Z* score ≤ −2 average: −1.1
Current OFC (cm) (*Z* score)	45.9 (-1.28)	52.2 (−2.6)	NR	N/A	52.3 (−1.02)	47.5 (−0.7)	48.7 (−1.2)	55.8 (+0.49)	NR	56.9 (+1.3)	NR	NR	53.5 (−0.76)	NR	1/13 (0%) with *Z* score ≤ −2 average: −0.72
Developmental delay and/or intellectual disability	+	+	+	N/A	+	+	+	+	+	+	+	+	+	+	13/13 (100%)
Speech and language	delayed	delayed	unknown	N/A	delayed	delayed	delayed	delayed	delayed	delayed	delayed	non-verbal	unknown	delayed	11/13 (85%)
Autism	–	–	–	N/A	+	N/A	–	+	unknown	+	+	+	–	–	5/12 (42%)

(*Continued on next page*)

Please cite this article in press as: Pan et al., *De novo* variants in *FRYL* are associated with developmental delay, intellectual disability, and dysmorphic features, The American Journal of Human Genetics (2024), https://doi.org/10.1016/j.ajhg.2024.02.007

Table 2. ***Continued***

	Individual 1	Individual 2	Individual 3	Individual 4	Individual 5	Individual 6	Individual 7	Individual 8	Individual 9	Individual 10	Individual 11	Individual 12	Individual 13	Individual 14	Summary
Psychiatric	–	dissociative motor disorder, borderline personality disorder, recurrent depressive disorders, eating disorder	–	N/A	poor socialization, avoidant/ restrictive food intake disorder (ARFID)	anxiety	–	ADHD	behavioral disturbances	tics	behavioral and sleep disturbances	unknown	adjustment disorder with depressed mood	ADHD	9/13 (69%)
Hypotonia	–	+	–	–	–	+	+	–	–	–	+	unknown	–	+	5/14 (36%)
Seizure	staring spells daily lasting 1–2 min	–	–	Seizures noted after cardiac arrest and prolonged hypotensive episode at 28 days. Recurrent seizure at 2 months. Right and left frontal and temporal sharps and rare spikes, poorly formed sleep architecture on EEG.	generalized epilepsy, onset age 2	–	–	–	focal seizures, epileptiform discharges in the right central region	–	–	–	–	–	4/14 (29%)
Brain MRI/CT findings	intraventricular hemorrhage and small subdural collections	normal	–	–	normal	–	normal	normal	mild thinning of the corpus callosum and mild diffuse cerebral volume loss	–	cortical dysplasia, incomplete inversion of the hippocampus	–	–	–	–
Cardiovascular	RV tumor, partial AVSD, ASD, PPS	PDA, PFO, pulmonary artery stenosis	TOF with PA	HLHS, AS, MS, LA egress obstruction, IAA	–	VSD, PPS	–	–	dextrocardia, common atrium, CAVC defect, IAA, PDA	–	–	–	dextrocardia, interrupted IVC, ASD, VSD, PDA	–	7/14 (50%)
Genitourinary	–	urinary incontinence	hydrocele	–	undescended testes, horseshoe kidney	hypospadias	–	–	hypospadias, undescended testes, chordee	–	–	–	–	undescended testes	6/14 (43%)
Gastrointestinal	–	–	–	jejunal atresia, microcolon	–	–	–	–	jejunal atresia, midline liver	–	–	–	midline liver, right-sided stomach	–	3/14 (21%)
Dysmorphic features	upslanting palpebral fissures, bitemporal narrowing, tall forehead, epicanthal folds, flat nasal bridge, short upturned nose, long well-grooved philtrum, cleft chin	long face, down-slanted palpebral fissures, retrognathy, low-set ears (can be attributed to *SF3B4* variant)	–	slightly triangular face, mild hypertelorism, low-set small ears with upturned lobules	sacral dimples, mildly anteverted nares	epicanthal folds, low nasal bridge, small ear tags, ear pit, nail dysplasia	frontal bossing, deep-set eyes, down-slanting palpebral fissure, nail dystrophy	deep-set eyes, up-slanting palpebral fissures, slightly posteriorly rotated ears	down-slanting palpebral fissures, flattened nasal bridge	deep-set eyes, up-slanting palpebral fissures, large ears, short philtrum	frontal bossing, anterior hairline	–	almond-shaped eyes, small hyperpigmented macule under right breast	–	11/14 (79%)

(*Continued on next page*)

Table 2. ***Continued***

	Individual 1	Individual 2	Individual 3	Individual 4	Individual 5	Individual 6	Individual 7	Individual 8	Individual 9	Individual 10	Individual 11	Individual 12	Individual 13	Individual 14	Summary
Additional phenotypes	pulmonary hypertension	hearing impairment, median cleft palate, dental crowding (can be attributed to *SF3B4* variant)	–	non-union of the sternum, unknown coagulopathy, chylous effusions	–	–	pectus carenatus, interstitial lung disease	–	unknown coagulopathy, spleen on right, polysplenia syndrome	–	–	–	dermatomyositis, stage 4B mixed cellularity Hodgkin lymphoma, functional asplenia	neonatal thrombocytopenia	–
Additional genetic test results	*PTPN11* VUS (c.879C>G [GenBank: NM_002834.5]; p.His293Gln), paternally inherited (asymptomatic father)	*de novo* pathogenic variant in *SF3B4* (c.417C>T [GenBank: NM_005850.5]; p.Asp140Leufs*3) for acrofacial dysostosis 1, Nager type, AD (MIM: 154400); (PVS1, PS2_Moderate, PS3, PS4_ Supporting, PM2_ Supporting); PS3 based on Cassina et al. and Wai et al.[24,25]	–	–	pathogenic variant in *DHCR7* (c.452G>A [GenBank: NM_ 001360.3]; p.Trp151*) for Smith-Lemli-Opitz syndrome, AR (MIM: 270400), maternally inherited	*de novo* VUS in maternal UPD 22	344 kb duplication in 19q13.41pat classified as likely benign	pathogenic variant in *SLC6A19* (c.1173 + 2T>G [GenBank: NM_001003841.3]) for Hartnup disorder, AR (MIM: 234500), heterozygous, maternally inherited	Heterozygous likely pathogenic variant in *DNAH11* (c.2152_ 2153delGT [GenBank: NM_ 001277115.2] p.Val718Glnfs*3) for PCD, AR (MIM: 617577), VUS in *FOXG1* (c.1425C>G [GenBank: NM_005249.4]; p.Phe475Leu), and 197 kb duplication at 10q21.3 classified as a VUS	likely benign variant in *ABCD1* (c.1447A>G [GenBank: NM_000033.3]; p.Thr483Ala) for X-linked adrenoleukodystrophy (MIM: 300100), maternally inherited, metabolic analysis normal (C26:0 Lyso PC and VLCFA)	–	–	VUS in *RSPH1* (c.916G>C [GenBank: NM_080860.2]; p.Asp306His) and VUS in *DNAH1* (c.11534G>T [GenBank: NM_ 001277115.1]; p.Arg3845Leu)	*de novo* heterozygous pathogenic variant in *SDHA* (c.223C>T [GenBank: NM_004168.4]; p.Arg75*) for pheochromocytoma and paraganglioma, AD (MIM: 614165)	–

Abbreviations: AD, autosomal dominant; ADHD, attention deficit hyperactivity disorder; AR, autosomal recessive; AS, aortic stenosis; ASD, atrial septal defect; AV, atrioventricular; AVSD, atrioventricular septal defect; CAVC, complete atrioventricular canal; EEG, electroencephalogram; HELLP, hemolysis, elevated liver enzymes, and low platelets; HLHS, hypoplastic left heart syndrome; IAA, interrupted aortic arch; IVC, inferior vena cava; LA, left atrium; LoF, loss of function; LSVC, left superior vena cava; LA, leftatrium; LV, left ventricle; MS, mitral stenosis; N/A, not applicable; NR, not reported; OT, occupational therapy; PA, pulmonary atresia; PC, phosphatidylcholine; PCD, primary ciliary dyskinesia PDA, patent ductus arteriosus; PFO, patent foramen ovale; PPS, peripheral pulmonary stenosis; PT, physical therapy; RA, right atrium; RV, right ventricle; TOF, tetralogy of fallot; UPD, uniparental disomy; VSD, ventricular septal defect; VUS, variant of uncertain significance.

Please cite this article in press as: Pan et al., *De novo* variants in *FRYL* are associated with developmental delay, intellectual disability, and dysmorphic features, The American Journal of Human Genetics (2024), https://doi.org/10.1016/j.ajhg.2024.02.007

The prime editing guide RNAs (pegRNAs) and nicking single-guide RNAs (sgRNA) were designed with the help from the PrimeDesign platform (http://primedesign.pinellolab.org/).[38] The pegRNAs were set to have 13 bp primer-binding sites (PBSs) and 16 bp reverse transcribed (RT) templates. All the protospacer adjacent motifs (PAMs) of the pegRNAs were disrupted by the edit to prevent repeated editing. To increase editing efficiency, second sgRNAs were designed to nick the opposite strand within 43 bp (for $fry^{p.Phe2024Leu}$) or 38 bp (for $fry^{p.Phe2746Ser}$) of the pegRNA-induced nicking. The pegRNA and nicking sgRNA sequences are listed in Table S3.

The pegRNA-tRNA-sgRNA sequences were synthesized and cloned into a pCFD5-white-NS vector by NEB HiFi Assembly (New England Biolabs) following the published cloning protocol.[37] The pCFD5-white-NS vector is modified from the pCFD5-NS vector (Addgene #149546) by replacing the vermillion selection marker by a *mini-white* sequence. Using the pCFD5-white-NS constructs, both pegRNA and sgRNA were expressed by a single *Drosophila* U6-3 promoter.[37,39] The constructs were injected into *vas-phiC31* embryos and inserted into the VK33 docking site using phiC31-mediated transgenesis.[40]

The induction of prime editing and the isolation of variant alleles were achieved following the published protocol.[37] The pegRNA-sgRNA-expressing flies were crossed to *nos-GAL4* u*pstream* a*ctivation sequence* ((*UAS*)-*PE2* flies to induce prime editing, and the progenies were cultured at 29°C and heat shocked at 37°C. In each trial, ten stocks were established for each variant, and flies with desired editing were selected by sequencing the modified locus using primers listed in Table S2. Two variants ($fry^{p.Phe2024Leu}$ and $fry^{p.Phe2746Ser}$) were successfully generated using this method in two trials. No successful editing was achieved for the other two variants ($fry^{p.Ser2910Ile}$ and $fry^{p.Tyr3410Cys}$), therefore an alternative method was employed (see below).

Generation of *fry* knockin lines by an RMCE- and single-strand annealing-based strategy

This gene knockin strategy is established based on previously developed methods.[41–43] All knockin alleles were successfully generated using this strategy. The schematic of the strategy is illustrated in Figure S2. All primers used in this protocol are listed in Table S2.

To generate the RMCE donor constructs, a 6.2 kb genomic sequence covering all the desired *fry* variants was amplified from the genomic DNA of $fry^{MI02265}$ flies using fry genomic primers. The genomic sequence was cloned in to a pDONR223 vector (Invitrogen) by BP cloning, and variants were introduced into the genomic sequence by Q5 site-directed mutagenesis (New England Biolabs). Following mutagenesis, the variant genomic sequences were amplified by PCR, and AatII and AscI sites were added. The PCR products were treated with AatII and AscI and ligated into AatII- and AscI-digested pTarget-RMCE vector (Drosophila Genomics Resource Center #1534).[41]

The donor constructs were injected into *vas-phiC31; ;* $fry^{MI02265}$ embryos where the donor sequences (6.2 kb genomic sequence plus *mini-white* marker) were swapped into the $fry^{MI02265}$ MiMIC site by RMCE. Successfully conversed flies ($fry^{MI02265\_RMCE}$) were selected by the loss of $yellow^{+}$ present in the MiMIC cassette and the gain of the $white^{+}$ present in the RMCE donor.[41,44] The correct orientation of the donor sequence was verified by PCR using the RMCE_ori primers.

Next, the $fry^{MI02265\text{-}RMCE}$ flies were crossed to the *hs-I-CreI* flies to induce double-strand breaks (DSBs) and the single-strand annealing (SSA) process (Figure S2). The expression of I-CreI was induced by heat shock at 37°C for 20 min. Potential variant alleles were isolated by selecting the $white^{-}$ flies. Ten stocks were isolated for each of the $fry^{p.Phe2024Leu}$, $fry^{p.Phe2746Ser}$, and $fry^{p.Ser2910Ile}$ variants, and fifteen stocks were isolated for the $fry^{p.Tyr3410Cys}$ variant. The correct variants ($fry^{Variant}$) were selected by sequencing the modified locus. In every case, we found at least one stock with the expected variant.

Immunofluorescence staining and confocal microscopy

Immunostaining of the larval CNS and adult brain samples was performed following a previously published method.[45] Briefly, samples were fixed in 4% paraformaldehyde for 1 h and washed in 0.2% Triton X-100 in PBS (PBT). Samples were next incubated with anti-Elav (DSHB #7E8A10; 1:500) or anti-Repo (DSHB #8D12; 1:50) antibody. Fluorescent secondary antibodies were used at 1:200 (Jackson ImmunoResearch). Finally, samples were clarified using RapidClear reagent (SUNJin lab) and mounted on slides. Confocal images of whole-mount samples were taken using a Zeiss LSM710 confocal microscope.

Drosophila behavioral assays

The fly behavioral assays were performed following previously published methods.[46,47] To measure negative geotaxis, flies were transferred to a clean vial for at least 20 min prior to the experiment. During the test, flies were tapped to the bottom of the vial and their negative geotaxis climbing ability was measured. In each measurement, flies were allowed to climb for 30 s, after which the climbing distances were measured (18 cm is maximum). To perform bang-sensitive paralytic analyses, adult flies were transferred to a clean vial and vortexed at maximum speed for 10 s, after which the time required for flies to stand on their feet was counted (30 s is maximum). To perform heat shock assay, flies were transferred to an empty vial and submerged in a 42°C water bath for 30 s. The percentage of flies that were unable to keep an upright position was quantified.

Developmental time course measurement

Flies were cultured in an egg laying cage for two days before embryo collection. Fly embryos were collected on grape juice plates supplemented with yeast paste every 2 h. Twenty-four hours after egg laying (AEL), the hatched L1 larvae with desired genotype were transferred to fly food. Thirty larvae were transferred to one culturing vial to avoid crowding during the culture. From 60 h AEL, newly molted L3 larvae were counted and then transferred to new fly food every 4 h. The time from embryo to L2-L3 molting was recorded. The L3 larvae were further cultured into pupae, and the number of newly formed pupae were recorded every 4 h until all larvae pupariated. The time from L2-L3 molting to pupariation was recorded. Since the timing of eclosion of *Drosophila* is largely influenced by the circadian clock,[48] the time course of eclosion was not recorded and studied.

Electroretinogram recording

Electroretinograms (ERGs) were recorded following an established method.[49] Briefly, flies were anesthetized by CO_2 and fixed to a slide with office glue. A recording electrode filled with 150 mM NaCl was placed on the surface of the compound eye and a ground electrode inserted into the upper torso. ERGs were recorded during pulses of light stimulation and later analyzed using the LabChart 8 software.

Please cite this article in press as: Pan et al., *De novo* variants in *FRYL* are associated with developmental delay, intellectual disability, and dysmorphic features, The American Journal of Human Genetics (2024), https://doi.org/10.1016/j.ajhg.2024.02.007

Statistical analysis

Statistical analyses were carried out using the Student's unpaired two-tailed t test for comparison of two groups. Multiple comparisons within the group were tested against the corresponding control. Calculated p values of less than 0.05 were considered significant. All statistical analyses were performed using GraphPad Prism, version 9.5.0 (GraphPad Software).

Results

Individuals with heterozygous variants in *FRYL* exhibit neurodevelopmental defects, dysmorphic facial features, and congenital anomalies

Fourteen unrelated individuals were found to harbor heterozygous variants in *FRYL* (GenBank: NM_015030.2). Thirteen out of the 14 variants were confirmed to be *de novo* and absent from gnomAD. The variant found in individual 13, c.7190G>T (p.Ser2397Ile), could not be confirmed *de novo* due to the lack of availability of the mother; however, the variant was not paternally inherited. This variant was present in gnomAD at a frequency of 4.02×10^{-6}. Population genetic data from the gnomAD database suggest that *FRYL* is intolerant to LoF (pLI = 1) and missense variants (Z score = 3.3). Moreover, only two individuals with a microdeletion covering coding exons of *FRYL* were documented in the Database of Genomic Variants (DGV). Among the 14 identified variants, nine are predicted LoF variants as they encode premature stop codons, frameshifts, or splicing defects. The five remaining are missense variants (Table 1). All the predicted LoF variants are predicted to undergo nonsense mediated decay (NMD).[50,51] All missense variants were predicted to be deleterious by multiple computational prediction tools, and all except the p.Ser2397Ile variant are classified as likely pathogenic by the ACMG/AMP guideline for variant interpretation (Table 1).[35]

The mapping locations of the missense variants are shown in Figure 1A. The affected amino acids are highly conserved across vertebrate species, and four out of five are conserved in *Drosophila* (Figure 1B). One missense variant, c.328C>T (p.Arg110Cys), which is not conserved in flies, is located within the FND, a highly evolutionarily conserved domain found in all Fry and Fryl proteins. Another missense variant, c.4882T>C (p.Phe1628Leu), maps to the central cell morphogenesis region, which is conserved across many proteins involved in the process of cell morphogenesis. The other three variants (c.6884T>C [p.Phe2295Ser], c.7190G>T [p.Ser2397Ile], and c.8852A>G [p.Tyr2951Cys]) do not map to known domains.

Clinical information about individuals with heterozygous *FRYL* variants is summarized in Table 2. The individuals include four females and nine males ranging in current age from 2.2 to 21 years, with a mean age of 11.3 years. Additionally, one male (individual 4) had a complex congenital heart disease (hypoplastic left heart syndrome [HLHS], aortic and mitral stenosis, left atrium egress obstruction, and interrupted aortic arch). He died at 4 months of age from cardiac failure and tachyarrhythmia secondary to hyperkalemia. This individual is included in the summary of features observed at birth but is excluded from the summary of non-congenital clinical features, such as autism, DD and/or intellectual disability, and behavioral differences, as he was not old enough at time of death to display these features.

Neurodevelopmental issues, including DD and/or intellectual disability, were observed in all 13 individuals in the cohort. A total of 10 individuals were noted to have delayed development of speech and language, and one other individual was non-verbal at 8 years of age (11/13, 85%). Autism spectrum disorder was observed in five individuals among those who were over the age of 3 and old enough to be diagnosed (5/12, 42%). Other behavioral challenges were reported in nine individuals (9/13, 69%), including attention deficit hyperactivity disorder (ADHD) in two individuals and general behavioral disturbances in two individuals, as well as dissociative motor disorder, borderline personality disorder, depressive disorders, eating disorder, poor socialization, anxiety, tics, and adjustment disorder with depressed mood in different individuals.

Five of the probands were noted to have hypotonia, and an additional three were noted to have a confirmed history of seizures. Individual 5 was diagnosed with generalized epilepsy at 2 years of age. Individual 9 had focal seizures with epileptiform discharges on electroencephalogram (EEG). Individual 4 had seizures after a prolonged hypotensive episode and cardiac arrest at 28 days of life, followed by another possible seizure at 2 months. This individual had epileptiform discharges on EEG at 2 months. A fourth individual, individual 1, had clinical seizure-like activity, with daily staring spells lasting 1–2 min, but has not yet had a diagnostic EEG. Among the six individuals who had neuroimaging (brain magnetic resonance imaging [MRI] or computed tomography [CT]), two had abnormal structural results. Individual 9 had mild thinning of the corpus callosum with mild diffuse cerebral volume loss, and individual 11 had cortical dysplasia.

The affected individuals were smaller than average at birth when adjusted for gestational age. The average Z score for birth length was −1.59, with one individual being significantly below average with a Z score of −4.7. At most recent follow-up visits, there was a trend toward shorter stature; the average Z score for current height was −1.1. Two individuals also had low birth weights with a Z score of ≤ -2, and four individuals (4/13, 31%) had a low weight (Z score ≤ -2) at their most recent visit.

Dysmorphic facial features were observed in a majority of individuals (11/14, 79%), with facial features of individuals 1 and 6 shown in Figure 2. Common facial features included upslanting (3/11) or downslanting palpebral fissures (3/11), deep-set eyes (3/11), epicanthal folds (2/11), flattened nasal bridge (3/11), and frontal bossing (2/11). Five individuals had variable ear features, including low-set ears, ear tags, slightly posteriorly rotated ears, and large ears.

Please cite this article in press as: Pan et al., *De novo* variants in *FRYL* are associated with developmental delay, intellectual disability, and dysmorphic features, The American Journal of Human Genetics (2024), https://doi.org/10.1016/j.ajhg.2024.02.007

Congenital heart defects were also common within the cohort (7/14, 50%). The congenital heart disease was often complex and required cardiac surgery (Table 2). There were two cases of heterotaxy syndrome. These probands were also both found to have a midline liver, and one had a right-sided spleen, whereas another had a right-sided stomach. Individual 1 was also diagnosed prenatally with a non-obstructive right ventricular tumor that has since regressed.

Other common features among these fourteen individuals included genitourinary and gastrointestinal abnormalities. Genitourinary abnormalities were reported in six individuals (6/14, 43%) and included undescended testes in three individuals, hypospadias in two individuals, and hydrocele, chordee, horseshoe kidney, and urinary incontinence. Gastrointestinal anomalies were seen in three individuals (21%). They include midline livers in the setting of heterotaxy syndrome, jejunal atresia, microcolon, and right-sided stomach.

Skeletal abnormalities of the chest were noted in two individuals: one with non-union of the sternum and the other with pectus carinatum. Two individuals were diagnosed with a coagulopathy of unknown etiology. Individual 13 had a history of stage 4B mixed cellularity Hodgkin lymphoma, which was in remission at the time of her most recent visit, as well as a history of dermatomyositis. Other medical issues observed in one individual each included: pulmonary hypertension, chylous effusions, interstitial lung disease, polysplenia syndrome, functional asplenia, and neonatal thrombocytopenia.

Two individuals in the cohort (individuals 2 and 14) were found to have *de novo* pathogenic variants in other disease-associated genes in addition to their variants in *FRYL*. Individual 2 was reported to have a *de novo* pathogenic variant in *SF3B4* (MIM: 605593), which is associated with autosomal dominant acrofacial dysostosis 1, otherwise known as Nager syndrome (MIM: 154400). This condition typically affects development of the face (down-slanted palpebral fissures, retrognathia, low-set ears, cleft palate, dental crowding observed in this individual) as well as pre-axial upper limb anomalies, such as radial hypoplasia or aplasia, small or absent thumbs, or radioulnar synostosis (none of which were observed in this individual).[52] Typically, individuals with Nager syndrome have normal cognitive function and normal cardiac structure, although there are occasional reports of individuals with Nager syndrome with congenital heart defects, such as patent ductus arteriosus, ventricular septal defect, or tetralogy of Fallot.[53] Individual 2 presented with intellectual disability, hypotonia, and congenital heart defects, which cannot be explained by the *SF3B4* variant. Individual 14 has a *de novo* pathogenic variant in *SDHA* (MIM: 600857) associated with an increased risk of pheochromocytoma and paraganglioma (MIM: 614165). However, *SDHA* is not associated with neurobehavioral phenotypes. Therefore, dual diagnoses were made for these two individuals.

Fly *fry* is the ortholog of human *FRYL*

To determine whether the *FRYL* variants are associated with the clinical features in the affected individuals, we used *Drosophila melanogaster* as the model organism. *Drosophila fry* is the ortholog of human *FRYL* and *FRY* with DIOPT scores[54] of 15/18 and 14/18, respectively. Fry and FRYL share 35% identity and 52% similarity (Figure S3). Most of the conserved domains in FRYL are also found in Fry, except for the leucine zipper/coiled-coil motifs (Figure 1A).[2] Among the five missense variants identified in the affected individuals, four (p.Phe1628Leu, p.Phe2295Ser, p.Ser2397Ile, and p.Tyr2951Cys) affect conserved amino acid residues in Fry, while the p.Arg110Cys variant affects a residue that is not conserved (Figure 1B).

Loss of *fry* causes lethality at an early developmental stage and morphological defects in mutant clones

Since most probands present with DD and various congenital anomalies, we first sought to determine whether *fry* is required for development. We first generated a $fry^{T2A\text{-}GAL4}$ allele by RMCE of a MiMIC insertion in $fry^{MI12326}$ allele (Figure 3A).[36,44,55,56] In this process, a splice acceptor (SA)-T2A-GAL4-polyA cassette is integrated in a coding intron shared by all *fry* transcripts.[55,57] The $fry^{T2A\text{-}GAL4}$ allele is predicted to be a severe loss-of-function (LoF) allele since the SA induces the inclusion of the artificial exon during transcription and the poly(A) sequence results in early transcription termination (Figure 3A).[57] We also used a previously reported fry^{1} allele, which is a null allele caused by a frameshift that affects amino acid 403 and beyond,[1] as well as a deficiency that encompasses *fry* (*Df(3L)BSC669*, marked as fry^{Df} hereafter).

Both fry^{1} homozygous and fry^{1}/fry^{Df} compound heterozygous mutations are lethal at the embryonic, L1, or L2 larval stages (Figure 3B). The $fry^{T2A\text{-}GAL4}$ allele fails to complement the fry^{1} and fry^{Df} alleles, and $fry^{T2A\text{-}GAL4}$ homozygous mutation is lethal at L2 and L3 larval or pupal stages (Figure 3B). These data suggest that $fry^{T2A\text{-}GAL4}$ is a strong LoF allele. The lethality associated with the $fry^{T2A\text{-}GAL4}$ homozygous mutation as well as the $fry^{T2A\text{-}GAL4}/fry^{1}$ and $fry^{T2A\text{-}GAL4}/fry^{Df}$ mutations is successfully rescued by a genomic rescue (GR) construct (*Dp(3:2)CH321-12N06*), which carries a copy of the *fry* locus[40] (Figure 3B). These data demonstrate that the defects are indeed caused by the loss of *fry* and show that *fry* is essential during development.

To study the requirement of *fry* in the development of different tissues, we generated fry^{1} homozygous clones in the wings and compound eyes using the FRT/FLP system.[58] We first generated clones in the wings using *ubx-FLP*. The cells in fry^{1} clones form clustered wing hairs, which contrasts with the neighboring heterozygous/wild-type cells that form a single hair on each cell (Figure 3C). This result is consistent with previous reports[1,6] and shows that the loss of *fry* causes defects in the development of the wing cells. In the compound eyes, we induced homozygous mutant clones using *ey-FLP*. The mutant clones are

Please cite this article in press as: Pan et al., *De novo* variants in *FRYL* are associated with developmental delay, intellectual disability, and dysmorphic features, The American Journal of Human Genetics (2024), https://doi.org/10.1016/j.ajhg.2024.02.007

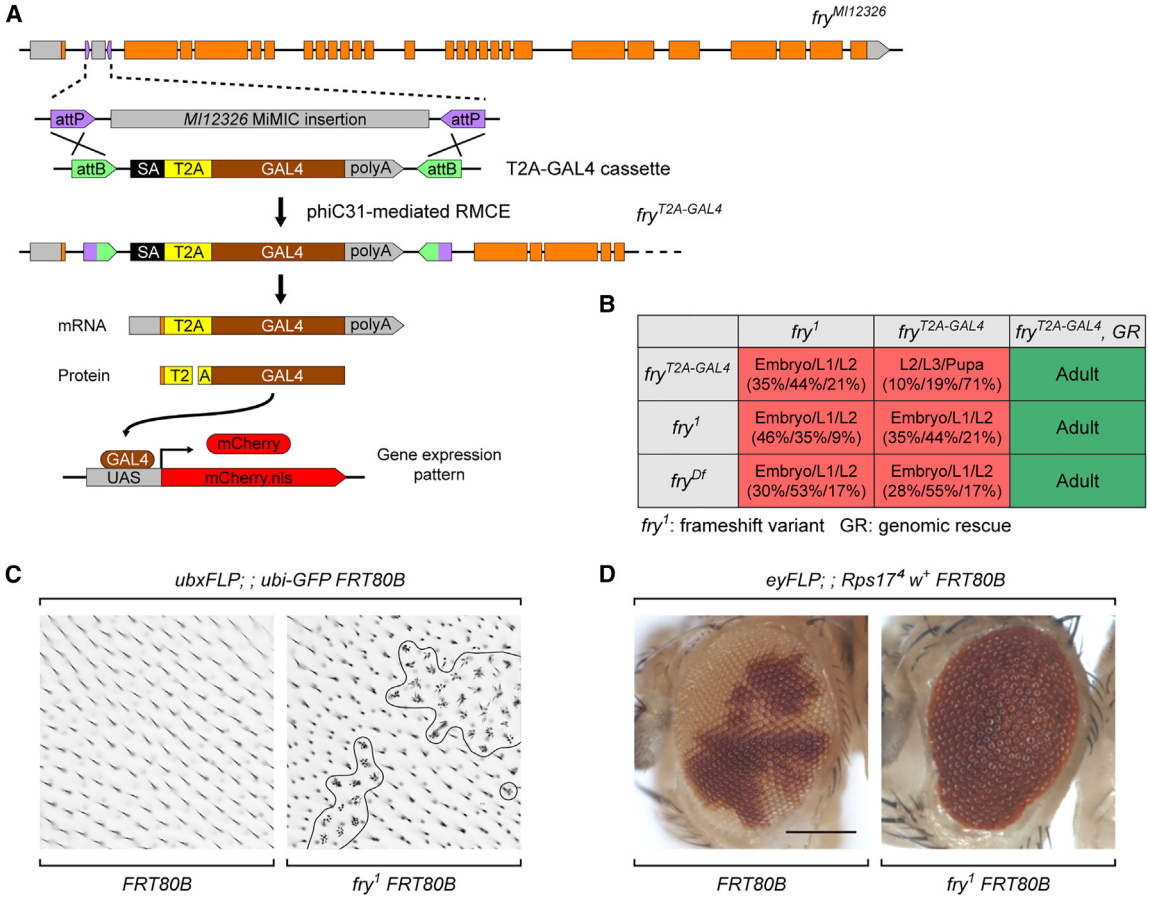

Figure 3. *Fry* is essential for fly development, and the loss of *fry* causes morphological defects in the wings and compound eyes
(A) Schematic of the generation of the $fry^{T2A\text{-}GAL4}$ allele. The $fry^{T2A\text{-}GAL4}$ allele is predicted to be a severe LoF allele. It also induces the expression of GAL4 protein under the control of the endogenous regulatory elements of *fry*, which can be used to determine the expression pattern using a fluorescent protein.
(B) Flies heterozygous for a severe LoF allele (fry^{1}) and a deficiency allele (fry^{Df}) are lethal at early developmental stages. The $fry^{T2A\text{-}GAL4}$ allele fails to complement both fry^{1} and fry^{Df} alleles. The stage-specific lethality rates are indicated in the table. Lethality caused by the loss of *fry* is rescued by the introduction of a genomic rescue (GR) construct.
(C) Fry^{1} homozygous mutant clones were generated in the fly wings using the FRT/FLP system. The loss of *fry* causes the clustered wing hair (furry) phenotype in clones.
(D) Fry^{1} homozygous mutant clones were generated in the fly compound eyes using the FRT/FLP system. Homozygous *fry* mutant clones are not present, and the eyes are small and rough, indicating that loss of *fry* causes cell lethality in the developing eye. Scale bar, 200 μm.

identified by their white color in contrast to the wild-type cells that are red. Normal eye size and smooth eye surface are observed when control *FRT80B* flies were used to generate clones (Figure 3D, left). In contrast, we did not observe homozygous mutant clones in the *ey-FLP; ; fry^{1} FRT80B/Rps17^4 w^{+} FRT80B* adult fly eyes. Moreover, the eyes with only wild-type cells are smaller and rough (Figure 3D, right), indicating that the homozygous mutant cells are eliminated during development.[59] This result shows that loss of *fry* disrupts eye development. Taken together, the results show that *fry* is essential for the development of multiple tissues.

Fry is predominantly expressed in neurons and localizes to the cytoplasm

FRYL is expressed in multiple tissues including the central nervous system (CNS) (GTEx).[60] Broad expression of *fry* is also observed in flies (FlyCellAtlas).[61] In the cohort, many individuals are affected by neurological deficits, including intellectual disability, autism, and seizures. Hence, we explored the expression pattern of *fry* in the fly CNS. The $fry^{T2A\text{-}GAL4}$ allele carries a T2A-GAL4 sequence, which induces the expression of the GAL4 transcription factor under the control of the endogenous regulatory elements of *fry*. The viral T2A sequence causes a skipping of the formation of peptide bond at the C-terminus of the T2A sequence during translation, leading to the production of untagged GAL4 (Figure 3A).[55,57] We examined *fry* expression pattern by crossing the $fry^{T2A\text{-}GAL4}$ allele to a *UAS-mCherry.nls* (nuclear-localized mCherry fluorescent protein). By co-staining with the pan-neuronal marker Elav or the pan-glial marker Repo, we found that the mCherry signals partially overlap with anti-Elav signals (Figure 4A), but not with the anti-Repo signals (Figure 4B)

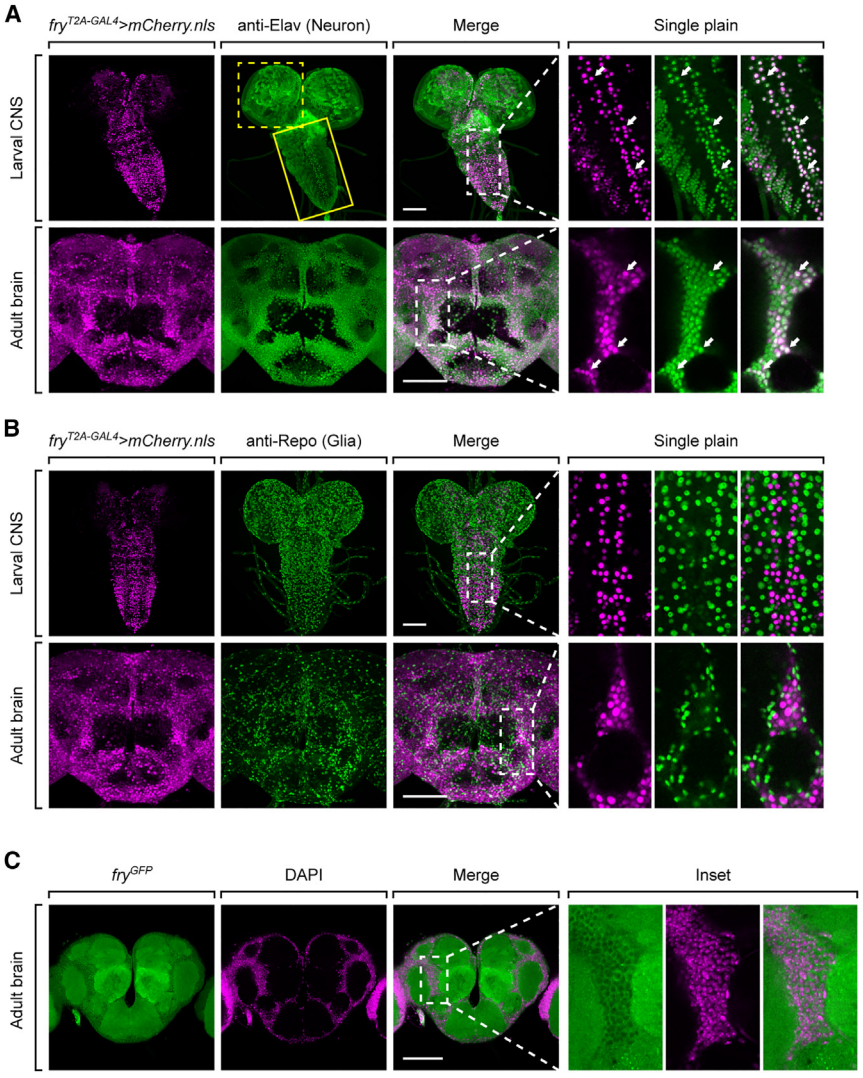

Figure 4. *Fry* is expressed in neurons in the fly CNS and localizes to the cytoplasm

(A and B) The expression of nuclear localized mCherry (mCherry.nls) was driven by the $fry^{T2A\text{-}GAL4}$ allele ($fry^{T2A\text{-}GAL4}$ > *mCherry.nls*). The larval CNS and adult brain of $fry^{T2A\text{-}GAL4}$ > *mCherry.nls* animals were immunostained with neuronal (Elav, A) or glial marker (Repo, B). Maximum projections of confocal z stack images are shown. *Fry* is expressed in neurons (A) but not in glia (B) in the fly CNS. In the larval CNS, *fry* is expressed more widely and strongly in the ventral nerve cord (yellow solid square) than in the brain lobes (yellow dashed square) (A). Single-plane, high magnification images of the regions indicated by the white dashed squares are shown on the right to visualize the co-localizations between mCherry and the immunostaining signals. Colocalizations are indicated by the arrows. Scale bars, 100 μm. (C) The localization of Fry in neurons was visualized by the GFP-tagged protein expressed by the fry^{GFP} allele. A single-plane image of the adult brain is shown. Fry localizes to the neuropil areas and the cytoplasm in the neuron bodies. Nuclei are marked by 4′,6-diamidino-2-phenylindole (DAPI) staining (magenta). High magnification images of the regions indicated by the white dashed squares are shown on the right to visualize the localization of Fryin the cell bodies. Scale bar, 100 μm.

in larval CNS and adult brains. Hence, *fry* is predominantly expressed in neurons but not in glia in the fly CNS. In the larval CNS, *fry* is expressed in a subset of neurons and the expression is wider and stronger in the ventral nerve cord than in the brain lobes. In the adult brain, *fry* is expressed in most neurons (Figure 4A). This expression pattern of *fry* is very similar to *para*, which encodes a voltage-gated sodium channel in flies.[62] *para* is only expressed in functionally active neurons, and most neurons in fly larvae (80%) are not active. Hence, *para* is expressed in a small subset of neurons in the larval CNS but is broadly expressed in the adult.[62] The expression pattern of *fry* suggests that *fry* is likely expressed in functionally active neurons. Given that human FRYL interacts with a nuclear-localized active form of NOTCH1,[19] we next examined the subcellular localization of Fry in the fly adult brains. To achieve this, we inserted an EGFP-FlAsH-StrepII-TEVcs-3xFLAG (GFSTF) cassette into the MiMIC site in the $fry^{MI12326}$ allele via RMCE.[56] The GFSTF sequence functions as an artificial exon,[56] which inserts a GFP tag in Fry (Figure S1). The resulting fry^{GFP} allele reverts the lethality caused by the MiMIC insertion and the fry^{GFP} homozygous animals are fully viable, indicating that the GFP tag does not disrupt protein function. As shown in Figure 4C, the GFP-tagged Fry proteins mainly localize to the cytoplasm of neuronal cell bodies as well as the neuropil in the adult brains.

Fry knockin alleles to study the effects of the human *FRYL* missense variants

To assess the function of the four *FRYL* missense variants, we generated *fry* gene knockin alleles by introducing analogous amino acid changes into the endogenous *fry* gene. Four *FRYL* variants, encoding p.Phe1628Leu, p.Phe2295Ser, p.Ser2397Ile, and p.Tyr2951Cys, correspond to the $fry^{p.Phe2024Leu}$, $fry^{p.Phe2746Ser}$, $fry^{p.Ser2910Ile}$, and $fry^{p.Tyr3410Cys}$ alleles, respectively. The FRYL p.Arg110Cys variant was not modeled as the affected residue is not conserved. The p.Ser2397Ile variant is found in the gnomAD database and the variant was not confirmed *de novo*. However, we modeled this variant since it is predicted to be deleterious by *in silico* algorithms (Table 1), and the affected residue is highly conserved across species (Figure 1B).

We first used the scarless prime editing (PE) method[37,63] (for details see material and methods) and were able to

A

	fry^{Df}	$fry^{T2A\text{-}GAL4}$	fry^{1}	fry^{1}, GR
$fry^{p.Phe2024Leu\_PE}$	Adult	Adult	Adult	Not tested
$fry^{p.Phe2746Ser\_PE}$	Embryo/L1/L2 (29%/60%/11%)	Embryo/L1/L2 (35%/47%/18%)	Embryo/L1/L2 (29%/52%/19%)	Adult
fry^{Ref_RMCE}	Adult	Adult	Adult	Not tested
$fry^{p.Phe2024Leu\_RMCE}$	Adult	Adult	Adult	Not tested
$fry^{p.Phe2746Ser\_RMCE}$	Embryo/L1/L2 (28%/50%/22%)	Embryo/L1/L2 (26%/53%/21%)	Embryo/L1/L2 (26%/59%/25%)	Adult
$fry^{p.Ser2910Ile\_RMCE}$	Adult	Adult	Adult	Not tested
$fry^{p.Tyr3410Cys\_RMCE}$	Adult	Adult	Adult	Not tested

GR: Genomic Rescue

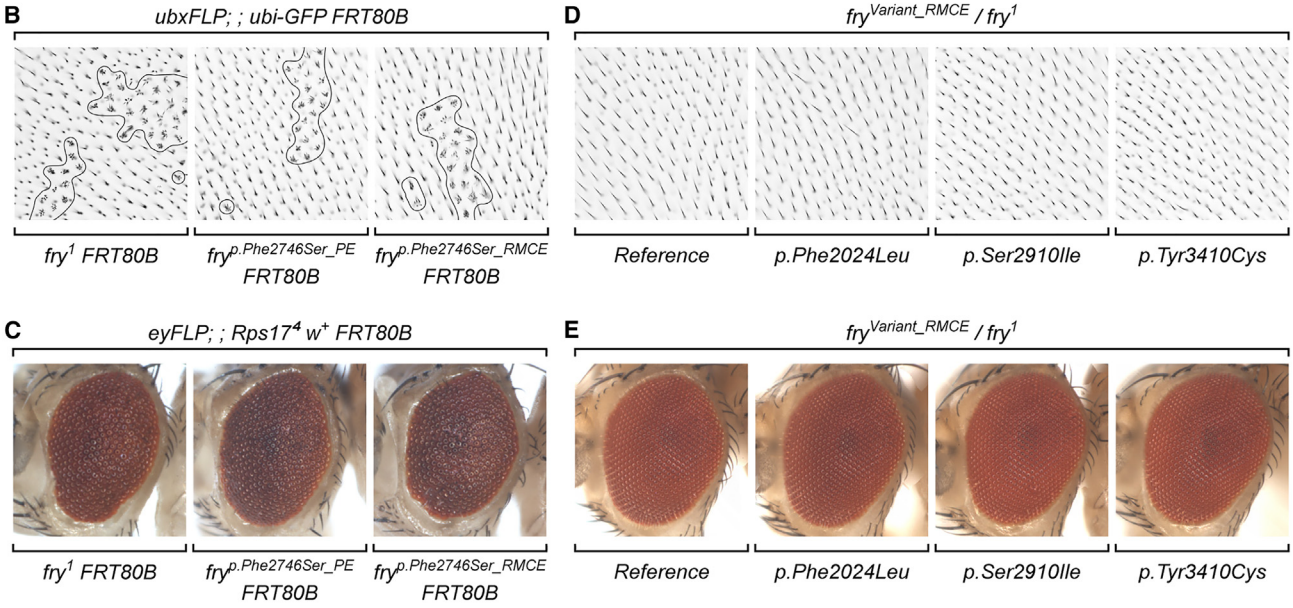

Figure 5. The *fry* p.Phe2746Ser variant, but not the other assayed variants, phenocopies severe LoF variants

(A) The *fry* p.Phe2746Ser variant (both PE and RMCE alleles) fails to complement the fry severe LoF variants, while the other three variants complement the severe LoF variants. The lethality of both $fry^{p.Phe2746Ser\_PE}/fry^{1}$ and $fry^{p.Phe2746Ser\_RMCE}/fry^{1}$ animals are rescued by the introduction of the genome rescue construct.

(B) *Fry* homozygous mutant clones were generated in the fly wings using the FRT/FLP system. Both $fry^{p.Phe2746Ser\_PE}$ and $fry^{p.Phe2746Ser\_RMCE}$ alleles cause clustered wing hair phenotype in the homozygous mutant clones, phenocopying the severe LoF fry^{1} allele.

(C) *Fry* homozygous mutant clones were generated in the fly compound eyes using the FRT/FLP system. Both $fry^{p.Phe2746Ser\_PE}$ and $fry^{p.Phe2746Ser\_RMCE}$ alleles cause cell lethality in the homozygous mutant clones as well as small and rough eyes, phenocopying the severe LoF fry^{1} allele.

(D) The wings of $fry^{p.Phe2024Leu\_RMCE}/fry^{1}$, $fry^{p.Ser2910Ile\_RMCE}/fry^{1}$, and $fry^{p.Tyr3410Cys\_RMCE}/fry^{1}$ flies do not exhibit clustered wing hair phenotype.

(E) The compound eyes of $fry^{p.Phe2024Leu\_RMCE}/fry^{1}$, $fry^{p.Ser2910Ile\_RMCE}/fry^{1}$, and $fry^{p.Tyr3410Cys\_RMCE}/fry^{1}$ flies do not exhibit any obvious morphological defect.

generate two alleles ($fry^{p.Phe2024Leu}$ and $fry^{p.Phe2746Ser}$) upon two trials. As we were not able to generate the other two alleles, we developed an alternative strategy, which is based on RMCE and SSA mechanisms and causes a small intronic insertion in *fry* (Figure S2).[41–43] This approach is clearly more efficient and allowed us to recover all four alleles upon the first trial. Hereafter, we denominate the nature of the alleles with PE and RMCE to refer to the corresponding method: for example, $fry^{p.Phe2024Leu\_PE}$ versus $fry^{p.Phe2024Leu\_RMCE}$. Since the RMCE-based method introduces a small intronic insertion, a fry^{WT_RMCE} control allele was generated, which has the same intronic insertion but no coding variant.

The *fry* p.Phe2746Ser variant phenocopies severe LoF variants

The *fry* alleles were first examined by complementation tests. Both $fry^{p.Phe2746Ser\_PE}$ and $fry^{p.Phe2746Ser\_RMCE}$ alleles fail to complement the fry^{1}, fry^{Df}, and $fry^{T2A\text{-}GAL4}$ alleles. The compound heterozygous animals die at the embryo/L1/L2 stages, and these animals are rescued by a GR construct (Figure 5A). We next tested the $fry^{p.Phe2746Ser}$ alleles in the wings and compound eyes. The $fry^{p.Phe2746Ser}$ homozygous wing clones lead to clustered wing hairs. It also causes aberrant compound eyes, which exhibit a rough eye phenotype and no visible homozygous clones (Figures 5B and 5C). These results show that both

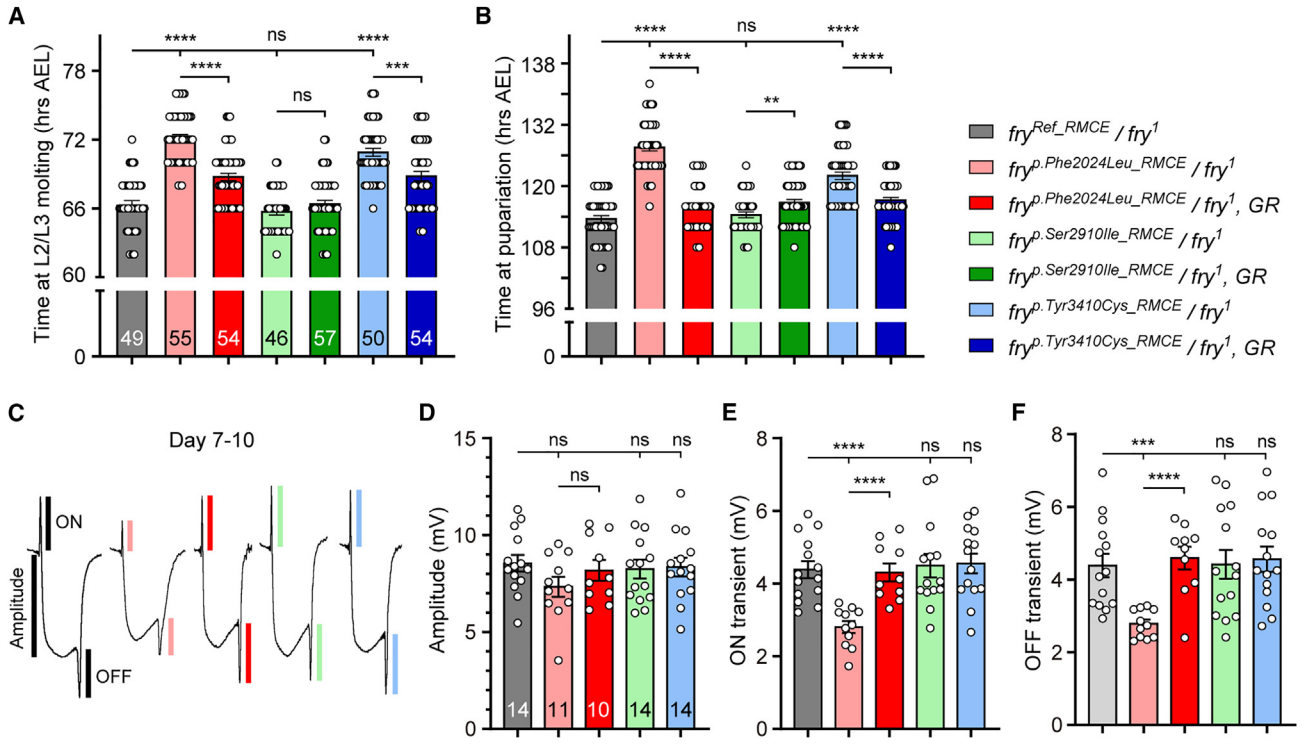

Figure 6. ***Fry*** **p.Phe2024Leu and p.Tyr3410Cys variants behave as partial LoF variants**

(A and B) The time courses from egg laying to L2/L3 molting (A) and to puparia formation (B) were measured in animals heterozygous for a tested missense allele and fry^{1} allele. Compared with the $fry^{p.WT\_RMCE}/fry^{1}$ controls, $fry^{p.Phe2024Leu\_RMCE}/fry^{1}$ and $fry^{p.Tyr3410Cys\_RMCE}/fry^{1}$ animals present with developmental delays in both measurements. The delays are rescued by the introduction of a genome rescue (GR) construct. The $fry^{p.Ser2910Ile\_RMCE}/fry^{1}$ animals do not show any delay in development.

(C–F) ERGs were recorded in animals heterozygous for a tested missense allele and fry^{1} allele (C). ON (D) and OFF (E) transients as well as amplitudes (F) were quantified. The ON and OFF transients in $fry^{p.Phe2024Leu\_RMCE}/fry^{1}$ flies significantly decrease compared with the control and GR construct rescues the decreases. In contrast, $fry^{p.Ser2910Ile\_RMCE}$ and $fry^{p.Tyr3410Cys\_RMCE}$ do not cause a significant change in ERG.

(A, B, and D–F) Results are presented as means ± SEM. Numbers of animals (n values) in each group are indicated under the bars. Results in (A) and (B), as well as results in (D–F), were obtained from the same samples. Statistical analyses were performed via unpaired Student's t test. ns, not significant; **$p < 0.01$; ***$p < 0.001$; ****$p < 0.0001$.

$fry^{p.Phe2746Ser}$ PE and RMCE alleles phenocopy the fry^{1} allele, suggesting that the p.Phe2746Ser variant causes a very severe LoF of Fry.

The *fry* p.Phe2024Leu and p.Tyr3410Cys variants behave as partial LoF variants

In contrast to the p.Phe2746Ser variant, the p.Phe2024Leu, p.Ser2910Ile, and p.Tyr3410Cys variants complement the lethality of the severe LoF alleles (Figure 5A) and do not cause obvious morphological defects in wings or compound eyes (Figures 5D and 5E). To determine whether these variants cause partial LoF effects, we crossed them to fry^{1} flies and assessed additional phenotypes in the compound heterozygous animals. Since the studied cohort presents with DD, we first measured the time courses of development from egg laying to L2/L3 molting and the formation of puparia. Compared with the fry^{WT_RMCE}/fry^{1} controls, the $fry^{p.Phe2024Leu\_RMCE}/fry^{1}$ and $fry^{p.Tyr3410Cys\_RMCE}/fry^{1}$ animals exhibit a significant developmental delay, and the delay is partially rescued by a GR construct. In contrast, the $fry^{p.Ser2910Ile\_RMCE}/fry^{1}$ animals do not show any delay (Figures 6A and 6B). Given that the loss of *fry* causes defects in eye development (Figure 3E) and that *fry* is expressed in adult photoreceptors (FlyCellAtlas, Figure S4),[61] we performed electroretinograms (ERGs) to assess whether the *fry* variants cause defects in neuronal activities. In an ERG (Figure 6C), the amplitude measures the activity of photoreceptors in response to photons upon light exposure, while the ON/OFF transients indicate the synaptic transmission between photoreceptors and the postsynaptic neurons.[64] We observed significantly reduced ON and OFF transients in the $fry^{p.Phe2024Leu\_RMCE}/fry^{1}$ flies, suggesting an impaired synaptic transmission. However, no significant change was observed in the amplitude (Figures 6C–6F). No ERG defect was observed in the $fry^{p.Ser2910Ile\_RMCE}/fry^{1}$ and $fry^{p.Tyr3410Cys\_RMCE}/fry^{1}$ animals (Figures 6C–6F).

Since some studied probands are affected by neurological deficits, we also explored other possible neurobehavioral phenotypes including locomotor activity and sensitivity to heat and physical stimulations and found that none of the variants cause obvious phenotypes in these assays (Figures S5A–S5C). Taken together, the results support that the *fry* p.Phe2024Leu and p.Tyr3410Cys variants

behave as partial LoF variants, although they are weak hypomorphs. In contrast, the p.Ser2910Ile variant is not associated with any phenotype in any assay, suggesting that the variant does not cause any detrimental effect in Fry.

Discussion

Here, we describe a cohort of fourteen unrelated individuals with heterozygous variants in *FRYL*. The most common clinical features were DD, intellectual disability, and facial dysmorphic features. Other features include neurobehavioral differences, autism spectrum disorder, hypotonia, and seizures, as well as congenital anomalies in cardiovascular, skeletal, gastrointestinal, renal, and urogenital systems. We provide human genetic evidence in combination with evidence from fruit flies that support that the variants correspond to LoF alleles. In this cohort, nine individuals are heterozygous for variants that lead to premature stop codons, frameshifts, or splicing defects. In a previous study, one individual with a *de novo* heterozygous variant (c.6121C>T [p.Arg2041*]) in the DDD cohort was identified who had short stature and craniofacial and cardiac defects, but no other information was provided.[22] In the ClinVar database, three frameshift variants and one splicing variant have been documented. The clinical features of the individuals with frameshift variants were not reported, while the individual with a heterozygous splicing variant had brisk reflexes, central hypotonia, central hypoventilation, delayed myelination, abnormal cerebral white matter morphology, and abnormal EEG (ClinVar accession: VCV001333288.1). The nine individuals reported in this study and the former two individuals described in DDD and ClinVar indicate that *FRYL* is haploinsufficient in humans. This is also supported by population genetic data from the gnomAD database that show that *FRYL* is intolerant to LoF (pLI = 1).

Five individuals in the studied cohort have a missense variant in *FRYL*. We modeled four out of the five variants, which share conserved amino acid residues in Fry, the fly ortholog of FRYL. By creating four *fry* knockin alleles, we assessed the effect of the missense variants in flies and showed that one variant (*fry* p.Phe2746Ser, analogous to *FRYL* p.Phe2295Ser) behaves as a severe LoF variant, whereas two variants (*fry* p.Phe2024Leu and p.Tyr3410Cys, analogous to *FRYL* p.Phe1628Leu and p.Tyr2951Cys, respectively) behave as partial LoF variants. The *fry* p.Ser2910Ile variant does not cause any phenotype in our fly assays. The corresponding *FRYL* p.Ser2397Ile variant is predicted to be pathogenic by multiple *in silico* algorithms. However, it is observed in gnomAD and was not confirmed *de novo* in the affected individual. Moreover, the affected individual is the only one in the cohort who did not present with DD. Due to the conflicting evidence, we argue that this variant is a variant of uncertain significance (VUS). This individual has a heterotaxy phenotype and may have variant(s) in a yet undescribed heterotaxy-associated gene. Without performing the same standardized quantitative assessments across the limited number of probands, it is difficult to compare the severity of phenotypes in the cohort, including the probands with the missense variants. The potential genotype-phenotype correlation could be studied in the future.

We frequently study human disease variants in fruit flies by integrating a *T2A-GAL4*[57,65] or Kozak-*GAL4*[66] to create a strong LoF allele. *GAL4* is expressed in the proper spatial and temporal expression pattern and typically allows to drive the UAS-human reference cDNA and rescue the LoF phenotypes in 50%–60% of the cases.[67] Unfortunately, a human *FRYL* cDNA is not available because the encoded protein is very large (3,013 amino acids); this is a common issue for large genes. Therefore, we generated the four *fry* knockin alleles in to allow the study of the human *FRYL* variants. Knockin animal models have been used to study genetic disorders caused by known pathogenic variants,[68–71] but the strategy used in these previous studies is very labor intensive and time consuming. Therefore, we first tried the recently developed PE methodology,[37,63] but we were only able to obtain two variants upon two trials. We then switched to an RMCE- and SSA-based mutagenesis strategy based on previously developed methods.[41–43] The latter approach allowed us to generate the four alleles in the first trial. Importantly, a visible marker (*white*$^{+}$) was employed for the selection of the positive lines in the RMCE-SSA strategy, which is not available in the PE strategy, and improved the selection process. Given that RMCE-compatible MiMIC or CRISPR-mediated integration cassette (CRIMIC) sites are available for ~7,000 genes,[44,56,65,66,72] this efficient gene knockin strategy can be used to assess many human variants.

Using established LoF alleles and knockin missense alleles analogous to human variants, we showed that *fry* is required for fly development, wing hair morphogenesis, and neuronal communication in the retina. Previous studies also showed that the loss of *fry* causes arborization defects of sensory dendrites,[7,8] supporting that *fry* plays a role in neural development. In a previous study, knock down of *fryl* in zebrafish causes cardiac and craniofacial defects during development.[22] These observations are not inconsistent with the observations that the individuals in the cohort have neuronal issues, including intellectual disability, autism spectrum disorder, and seizures, as well as defects in morphogenesis in multiple organs. However, additional experiments will be required in model organisms to assess the roles of the *Furry* genes and their linkage to the human phenotypes.

Humans have two Furry proteins, FRYL and FRY. Although the homology between the two paralogs is significant, the functional redundancy between these genes is not. Biallelic variants in *FRY* have been observed in individuals with intellectual disability in three consanguineous families.[15–17] Intellectual disability is also observed in 8/13 individuals in the studied cohort. However, no other *FRYL*-associated phenotypes were reported in the

individuals with *FRY* variants. Homozygous *Fryl* mutant mice present with developmental retardation and kidney developmental defects, but these animals were not assessed for neurological issues and most of the animals died soon after birth.[21] *Fry* mutant mice were reported in one forward genetic screen for defects in skeletal development. Mice homozygous for a frameshift *Fry* variant present with reduced tibia, femur, and pelvis lengths. However, no other phenotypic information was reported.[73] In the cohort reported here, a renal abnormality was reported in one individual (horseshoe kidney in individual 5), while skeletal defects were observed in two individuals (nonunion of the sternum in individual 4 and pectus carinatum in individual 7). The molecular functions of mammalian Furry proteins are largely unknown. In non-mammalian model organisms, the best characterized activity of Furry proteins is their interactions with NDR (nuclear dbf2-related) family kinases in multiple species.[1,2,4–7] In flies, loss of an NDR kinase *tricornered* (*trc*) phenocopies *fry* mutants in dendritic tiling and wing hair development, providing evidence that both genes play a role in the same pathway.[6,7] Similar genetic and physical interactions have also been reported in yeasts and worms.[2,4,5] In humans, FRY interacts with the NDR kinase NDR1 to regulate chromosome alignment during mitosis.[10] However, it is not known whether FRYL interacts with NDR kinases. The NDR1/2 encoding genes *STK38* (MIM: 606964) and *STK38L* (MIM: 615836) have not yet been associated with inherited disorders. Both *Stk38* and *Stk38l* homozygous mutant mice are viable[74,75] but show defects in retina development,[76] indicating a functional redundancy. *Stk38l* mutant mice also show abnormal dendrite morphology in neurons, consistent with the findings in flies that the loss of fly NDR (Trc) causes defects in dendritic tiling.[75] In summary, studies focusing on the biological functions of FRYL during development will provide a better understanding of the mechanisms underlying disease pathogenesis.

Consortia

The members of the Center for Precision Medicine Models (CPMM) at Baylor College of Medicine are Lindsay C. Burrage, Jason D. Heaney, Seon-Young Kim, Denise G. Lanza, Zhandong Liu, Dongxue Mao, Aleksander Milosavljevic, Sandesh C.S. Nagamani, Jennifer E. Posey, Uma Ramamurthy, Vivek Ramanathan, Jeffrey Rogers, Jill A. Rosenfeld, Matthew Roth, and Ramin Zahedi Darshoori.

Data and code availability

All reagents developed in this study are available upon request. The exome datasets supporting this study have not been deposited to a public database due to privacy issues. We cannot release the full exomes/genomes because the condition is so rare and the clinical characteristics so specific that the participants could be identifiable.

Supplemental information

Supplemental information can be found online at https://doi.org/10.1016/j.ajhg.2024.02.007.

Acknowledgments

We thank the participants and their families for supporting this study. We thank the Bellen and Yamamoto lab members for their discussion and suggestions. We thank Ms. Wen-Wen Lin, Ying Fang, and Junyan Fang for fly embryo injection. We thank the BDSC for fly stocks, the DSHB for antibodies, and the DGRC for plasmids.

H.J.B., S.Y., and O.K. are members of the CPMM. The CPMM was supported by the Office of Research Infrastructure Programs (ORIP) of the NIH (award U54OD030165). H.J.B. was supported by the ORIP (award R24OD031447), the Huffington Foundation, and the Duncan Neurological Research Institute at Texas Children's Hospital. The work was also supported by the Baylor College of Medicine IDDRC (P50HD103555) from the Eunice Kennedy Shriver National Institute of Child Health and Human Development of the NIH for use of the Microscopy Core facilities. W.K.C. was supported by the National Heart, Lung, and Blood Institute (NHLBI) of the NIH (award U01HL131003). A.R.-P. was supported by the National Center for Advancing Translational Sciences of the NIH (award UL1TR001873). L.O. and D.A.S. were supported by the American Institute for Neuro-Integrative Development (AIND) and The Hill Family Fund for the Diagnosis, Management of Rare and Undiagnosed Diseases at Mass General. The content is solely the responsibility of the authors and does not necessarily represent the official views of the NIH. A.P.A.S. and M.S. are members of the European Reference Network on Rare Congenital Malformations and Rare Intellectual Disability ERN-ITHACA (EU Framework Partnership agreement ID: 3HP-HP-FPA ERN-01-2016/739516).

Declaration of interests

W.K.C. is a member of the Board of Directors of Prime Medicine and RallyBio. R.P. is an employee of GeneDx, LLC.

Received: August 23, 2023
Accepted: February 12, 2024
Published: March 12, 2024

Web resources

CADD, https://cadd.gs.washington.edu/
ClinVar, https://www.ncbi.nlm.nih.gov/clinvar/
DGV, http://dgv.tcag.ca/
DIOPT, http://www.flyrnai.org/diopt/
FlyCellAtlas, https://scope.aertslab.org/#/FlyCellAtlas/
gnomAD, https://gnomad.broadinstitute.org/
GTEx, https://gtexportal.org/
M-CAP, http://bejerano.stanford.edu/mcap/
MutationTaster, http://www.mutationtaster.org/
OMIM, https://omim.org/
PolyPhen2, http://genetics.bwh.harvard.edu/pph2/
PROVEAN, https://www.jcvi.org/research/provean/
REVEL, https://sites.google.com/site/revelgenomics/
SIFT, https://sift.bii.a-star.edu.sg/

References

1. Cong, J., Geng, W., He, B., Liu, J., Charlton, J., and Adler, P.N. (2001). The furry gene of Drosophila is important for maintaining the integrity of cellular extensions during morphogenesis. Development *128*, 2793–2802. https://doi.org/10.1242/dev.128.14.2793.
2. Gallegos, M.E., and Bargmann, C.I. (2004). Mechanosensory neurite termination and tiling depend on SAX-2 and the SAX-1 kinase. Neuron *44*, 239–249. https://doi.org/10.1016/j.neuron.2004.09.021.
3. Goto, T., Fukui, A., Shibuya, H., Keller, R., and Asashima, M. (2010). Xenopus furry contributes to release of microRNA gene silencing. Proc. Natl. Acad. Sci. USA *107*, 19344–19349. https://doi.org/10.1073/pnas.1008954107.
4. Hirata, D., Kishimoto, N., Suda, M., Sogabe, Y., Nakagawa, S., Yoshida, Y., Sakai, K., Mizunuma, M., Miyakawa, T., Ishiguro, J., and Toda, T. (2002). Fission yeast Mor2/Cps12, a protein similar to Drosophila Furry, is essential for cell morphogenesis and its mutation induces Wee1-dependent G(2) delay. EMBO J. *21*, 4863–4874. https://doi.org/10.1093/emboj/cdf495.
5. Du, L.L., and Novick, P. (2002). Pag1p, a novel protein associated with protein kinase Cbk1p, is required for cell morphogenesis and proliferation in Saccharomyces cerevisiae. Mol. Biol. Cell *13*, 503–514. https://doi.org/10.1091/mbc.01-07-0365.
6. He, Y., Fang, X., Emoto, K., Jan, Y.N., and Adler, P.N. (2005). The tricornered Ser/Thr protein kinase is regulated by phosphorylation and interacts with furry during Drosophila wing hair development. Mol. Biol. Cell *16*, 689–700. https://doi.org/10.1091/mbc.e04-09-0828.
7. Emoto, K., He, Y., Ye, B., Grueber, W.B., Adler, P.N., Jan, L.Y., and Jan, Y.N. (2004). Control of dendritic branching and tiling by the Tricornered-kinase/Furry signaling pathway in Drosophila sensory neurons. Cell *119*, 245–256. https://doi.org/10.1016/j.cell.2004.09.036.
8. Han, C., Wang, D., Soba, P., Zhu, S., Lin, X., Jan, L.Y., and Jan, Y.N. (2012). Integrins regulate repulsion-mediated dendritic patterning of drosophila sensory neurons by restricting dendrites in a 2D space. Neuron *73*, 64–78. https://doi.org/10.1016/j.neuron.2011.10.036.
9. Mistry, J., Chuguransky, S., Williams, L., Qureshi, M., Salazar, G.A., Sonnhammer, E.L.L., Tosatto, S.C.E., Paladin, L., Raj, S., Richardson, L.J., et al. (2021). Pfam: The protein families database in 2021. Nucleic Acids Res. *49*, D412–D419. https://doi.org/10.1093/nar/gkaa913.
10. Chiba, S., Ikeda, M., Katsunuma, K., Ohashi, K., and Mizuno, K. (2009). MST2- and Furry-mediated activation of NDR1 kinase is critical for precise alignment of mitotic chromosomes. Curr. Biol. *19*, 675–681. https://doi.org/10.1016/j.cub.2009.02.054.
11. Ikeda, M., Chiba, S., Ohashi, K., and Mizuno, K. (2012). Furry protein promotes aurora A-mediated Polo-like kinase 1 activation. J. Biol. Chem. *287*, 27670–27681. https://doi.org/10.1074/jbc.M112.378968.
12. Nagai, T., Ikeda, M., Chiba, S., Kanno, S.I., and Mizuno, K. (2013). Furry promotes acetylation of microtubules in the mitotic spindle by inhibition of SIRT2 tubulin deacetylase. J. Cell Sci. *126*, 4369–4380. https://doi.org/10.1242/jcs.127209.
13. Mai, Z., Yuan, J., Yang, H., Fang, S., Xie, X., Wang, X., Xie, J., Wen, J., and Fu, J. (2022). Inactivation of Hippo pathway characterizes a poor-prognosis subtype of esophageal cancer. JCI Insight *7*, e155218. https://doi.org/10.1172/jci.insight.155218.
14. Ren, X., Graham, J.C., Jing, L., Mikheev, A.M., Gao, Y., Lew, J.P., Xie, H., Kim, A.S., Shang, X., Friedman, C., et al. (2013). Mapping of Mcs30, a new mammary carcinoma susceptibility quantitative trait locus (QTL30) on rat chromosome 12: identification of fry as a candidate Mcs gene. PLoS One *8*, e70930. https://doi.org/10.1371/journal.pone.0070930.
15. Najmabadi, H., Hu, H., Garshasbi, M., Zemojtel, T., Abedini, S.S., Chen, W., Hosseini, M., Behjati, F., Haas, S., Jamali, P., et al. (2011). Deep sequencing reveals 50 novel genes for recessive cognitive disorders. Nature *478*, 57–63. https://doi.org/10.1038/nature10423.
16. Paulraj, P., Bosworth, M., Longhurst, M., Hornbuckle, C., Gotway, G., Lamb, A.N., and Andersen, E.F. (2019). A Novel Homozygous Deletion within the FRY Gene Associated with Nonsyndromic Developmental Delay. Cytogenet. Genome Res. *159*, 19–25. https://doi.org/10.1159/000502598.
17. Riazuddin, S., Hussain, M., Razzaq, A., Iqbal, Z., Shahzad, M., Polla, D.L., Song, Y., van Beusekom, E., Khan, A.A., Tomas-Roca, L., et al. (2017). Exome sequencing of Pakistani consanguineous families identifies 30 novel candidate genes for recessive intellectual disability. Mol. Psychiatr. *22*, 1604–1614. https://doi.org/10.1038/mp.2016.109.
18. Hayette, S., Cornillet-Lefebvre, P., Tigaud, I., Struski, S., Forissier, S., Berchet, A., Doll, D., Gillot, L., Brahim, W., Delabesse, E., et al. (2005). AF4p12, a human homologue to the furry gene of Drosophila, as a novel MLL fusion partner. Cancer Res. *65*, 6521–6525. https://doi.org/10.1158/0008-5472.CAN-05-1325.
19. Yatim, A., Benne, C., Sobhian, B., Laurent-Chabalier, S., Deas, O., Judde, J.G., Lelievre, J.D., Levy, Y., and Benkirane, M. (2012). NOTCH1 nuclear interactome reveals key regulators of its transcriptional activity and oncogenic function. Mol. Cell *48*, 445–458. https://doi.org/10.1016/j.molcel.2012.08.022.
20. Grabher, C., von Boehmer, H., and Look, A.T. (2006). Notch 1 activation in the molecular pathogenesis of T-cell acute lymphoblastic leukaemia. Nat. Rev. Cancer *6*, 347–359. https://doi.org/10.1038/nrc1880.
21. Byun, Y.S., Kim, E.K., Araki, K., Yamamura, K.I., Lee, K., Yoon, W.K., Won, Y.S., Kim, H.C., Choi, K.C., and Nam, K.H. (2018). Fryl deficiency is associated with defective kidney development and function in mice. Exp. Biol. Med. *243*, 408–417. https://doi.org/10.1177/1535370218758249.
22. Deciphering Developmental Disorders Study (2015). Large-scale discovery of novel genetic causes of developmental disorders. Nature *519*, 223–228. https://doi.org/10.1038/nature14135.
23. Sobreira, N., Schiettecatte, F., Valle, D., and Hamosh, A. (2015). GeneMatcher: a matching tool for connecting investigators with an interest in the same gene. Hum. Mutat. *36*, 928–930. https://doi.org/10.1002/humu.22844.
24. Cassina, M., Cerqua, C., Rossi, S., Salviati, L., Martini, A., Clementi, M., and Trevisson, E. (2017). A synonymous splicing mutation in the SF3B4 gene segregates in a family with highly variable Nager syndrome. Eur. J. Hum. Genet. *25*, 371–375. https://doi.org/10.1038/ejhg.2016.176.
25. Wai, H.A., Lord, J., Lyon, M., Gunning, A., Kelly, H., Cibin, P., Seaby, E.G., Spiers-Fitzgerald, K., Lye, J., Ellard, S., et al. (2020). Blood RNA analysis can increase clinical diagnostic rate and resolve variants of uncertain significance. Genet. Med. *22*, 1005–1014. https://doi.org/10.1038/s41436-020-0766-9.

26. Karczewski, K.J., Francioli, L.C., Tiao, G., Cummings, B.B., Alföldi, J., Wang, Q., Collins, R.L., Laricchia, K.M., Ganna, A., Birnbaum, D.P., et al. (2020). The mutational constraint spectrum quantified from variation in 141,456 humans. Nature *581*, 434–443. https://doi.org/10.1038/s41586-020-2308-7.
27. Adzhubei, I.A., Schmidt, S., Peshkin, L., Ramensky, V.E., Gerasimova, A., Bork, P., Kondrashov, A.S., and Sunyaev, S.R. (2010). A method and server for predicting damaging missense mutations. Nat. Methods *7*, 248–249. https://doi.org/10.1038/nmeth0410-248.
28. Schwarz, J.M., Rödelsperger, C., Schuelke, M., and Seelow, D. (2010). MutationTaster evaluates disease-causing potential of sequence alterations. Nat. Methods *7*, 575–576. https://doi.org/10.1038/nmeth0810-575.
29. Kumar, P., Henikoff, S., and Ng, P.C. (2009). Predicting the effects of coding non-synonymous variants on protein function using the SIFT algorithm. Nat. Protoc. *4*, 1073–1081. https://doi.org/10.1038/nprot.2009.86.
30. Choi, Y., and Chan, A.P. (2015). PROVEAN web server: a tool to predict the functional effect of amino acid substitutions and indels. Bioinformatics *31*, 2745–2747. https://doi.org/10.1093/bioinformatics/btv195.
31. Choi, Y., Sims, G.E., Murphy, S., Miller, J.R., and Chan, A.P. (2012). Predicting the functional effect of amino acid substitutions and indels. PLoS One *7*, e46688. https://doi.org/10.1371/journal.pone.0046688.
32. Kircher, M., Witten, D.M., Jain, P., O'Roak, B.J., Cooper, G.M., and Shendure, J. (2014). A general framework for estimating the relative pathogenicity of human genetic variants. Nat. Genet. *46*, 310–315. https://doi.org/10.1038/ng.2892.
33. Ioannidis, N.M., Rothstein, J.H., Pejaver, V., Middha, S., McDonnell, S.K., Baheti, S., Musolf, A., Li, Q., Holzinger, E., Karyadi, D., et al. (2016). REVEL: An Ensemble Method for Predicting the Pathogenicity of Rare Missense Variants. Am. J. Hum. Genet. *99*, 877–885. https://doi.org/10.1016/j.ajhg.2016.08.016.
34. Jagadeesh, K.A., Wenger, A.M., Berger, M.J., Guturu, H., Stenson, P.D., Cooper, D.N., Bernstein, J.A., and Bejerano, G. (2016). M-CAP eliminates a majority of variants of uncertain significance in clinical exomes at high sensitivity. Nat. Genet. *48*, 1581–1586. https://doi.org/10.1038/ng.3703.
35. Richards, S., Aziz, N., Bale, S., Bick, D., Das, S., Gastier-Foster, J., Grody, W.W., Hegde, M., Lyon, E., Spector, E., et al. (2015). Standards and guidelines for the interpretation of sequence variants: a joint consensus recommendation of the American College of Medical Genetics and Genomics and the Association for Molecular Pathology. Genet. Med. *17*, 405–424. https://doi.org/10.1038/gim.2015.30.
36. Nagarkar-Jaiswal, S., DeLuca, S.Z., Lee, P.T., Lin, W.W., Pan, H., Zuo, Z., Lv, J., Spradling, A.C., and Bellen, H.J. (2015). A genetic toolkit for tagging intronic MiMIC containing genes. Elife *4*, e08469. https://doi.org/10.7554/eLife.08469.
37. Bosch, J.A., Birchak, G., and Perrimon, N. (2021). Precise genome engineering in Drosophila using prime editing. Proc. Natl. Acad. Sci. USA *118*, e2021996118. https://doi.org/10.1073/pnas.2021996118.
38. Hsu, J.Y., Grünewald, J., Szalay, R., Shih, J., Anzalone, A.V., Lam, K.C., Shen, M.W., Petri, K., Liu, D.R., Joung, J.K., and Pinello, L. (2021). PrimeDesign software for rapid and simplified design of prime editing guide RNAs. Nat. Commun. *12*, 1034. https://doi.org/10.1038/s41467-021-21337-7.
39. Port, F., Chen, H.M., Lee, T., and Bullock, S.L. (2014). Optimized CRISPR/Cas tools for efficient germline and somatic genome engineering in Drosophila. Proc. Natl. Acad. Sci. USA *111*, E2967–E2976. https://doi.org/10.1073/pnas.1405500111.
40. Venken, K.J.T., He, Y., Hoskins, R.A., and Bellen, H.J. (2006). P[acman]: a BAC transgenic platform for targeted insertion of large DNA fragments in D. melanogaster. Science *314*, 1747–1751. https://doi.org/10.1126/science.1134426.
41. Feng, S., Lu, S., Grueber, W.B., and Mann, R.S. (2021). Scarless engineering of the Drosophila genome near any site-specific integration site. Genetics *217*, iyab012. https://doi.org/10.1093/genetics/iyab012.
42. Garcia-Marques, J., Yang, C.P., Espinosa-Medina, I., Mok, K., Koyama, M., and Lee, T. (2019). Unlimited Genetic Switches for Cell-Type-Specific Manipulation. Neuron *104*, 227–238.e7. https://doi.org/10.1016/j.neuron.2019.07.005.
43. Vilain, S., Vanhauwaert, R., Maes, I., Schoovaerts, N., Zhou, L., Soukup, S., da Cunha, R., Lauwers, E., Fiers, M., and Verstreken, P. (2014). Fast and efficient Drosophila melanogaster gene knock-ins using MiMIC transposons. G3 (Bethesda) *4*, 2381–2387. https://doi.org/10.1534/g3.114.014803.
44. Venken, K.J.T., Schulze, K.L., Haelterman, N.A., Pan, H., He, Y., Evans-Holm, M., Carlson, J.W., Levis, R.W., Spradling, A.C., Hoskins, R.A., and Bellen, H.J. (2011). MiMIC: a highly versatile transposon insertion resource for engineering Drosophila melanogaster genes. Nat. Methods *8*, 737–743. https://doi.org/10.1038/nmeth.1662.
45. Accogli, A., Lu, S., Musante, I., Scudieri, P., Rosenfeld, J.A., Severino, M., Baldassari, S., Iacomino, M., Riva, A., Balagura, G., et al. (2023). Loss of Neuron Navigator 2 Impairs Brain and Cerebellar Development. Cerebellum *22*, 206–222. https://doi.org/10.1007/s12311-022-01379-3.
46. Lu, S., Hernan, R., Marcogliese, P.C., Huang, Y., Gertler, T.S., Akcaboy, M., Liu, S., Chung, H.L., Pan, X., Sun, X., et al. (2022). Loss-of-function variants in TIAM1 are associated with developmental delay, intellectual disability, and seizures. Am. J. Hum. Genet. *109*, 571–586. https://doi.org/10.1016/j.ajhg.2022.01.020.
47. Lu, S., Ma, M., Mao, X., Bacino, C.A., Jankovic, J., Sutton, V.R., Bartley, J.A., Wang, X., Rosenfeld, J.A., Beleza-Meireles, A., et al. (2022). De novo variants in FRMD5 are associated with developmental delay, intellectual disability, ataxia, and abnormalities of eye movement. Am. J. Hum. Genet. *109*, 1932–1943. https://doi.org/10.1016/j.ajhg.2022.09.005.
48. Qiu, J., and Hardin, P.E. (1996). Developmental state and the circadian clock interact to influence the timing of eclosion in Drosophila melanogaster. J. Biol. Rhythm. *11*, 75–86. https://doi.org/10.1177/074873049601100108.
49. Verstreken, P., Koh, T.W., Schulze, K.L., Zhai, R.G., Hiesinger, P.R., Zhou, Y., Mehta, S.Q., Cao, Y., Roos, J., and Bellen, H.J. (2003). Synaptojanin is recruited by endophilin to promote synaptic vesicle uncoating. Neuron *40*, 733–748. https://doi.org/10.1016/s0896-6273(03)00644-5.
50. Holbrook, J.A., Neu-Yilik, G., Hentze, M.W., and Kulozik, A.E. (2004). Nonsense-mediated decay approaches the clinic. Nat. Genet. *36*, 801–808. https://doi.org/10.1038/ng1403.
51. Supek, F., Lehner, B., and Lindeboom, R.G.H. (2021). To NMD or Not To NMD: Nonsense-Mediated mRNA Decay in Cancer and Other Genetic Diseases. Trends Genet. *37*, 657–668. https://doi.org/10.1016/j.tig.2020.11.002.

52. Bernier, F.P., Caluseriu, O., Ng, S., Schwartzentruber, J., Buckingham, K.J., Innes, A.M., Jabs, E.W., Innis, J.W., Schuette, J.L., Gorski, J.L., et al. (2012). Haploinsufficiency of SF3B4, a component of the pre-mRNA spliceosomal complex, causes Nager syndrome. Am. J. Hum. Genet. *90*, 925–933. https://doi.org/10.1016/j.ajhg.2012.04.004.
53. Petit, F., Escande, F., Jourdain, A.S., Porchet, N., Amiel, J., Doray, B., Delrue, M.A., Flori, E., Kim, C.A., Marlin, S., et al. (2014). Nager syndrome: confirmation of SF3B4 haploinsufficiency as the major cause. Clin. Genet. *86*, 246–251. https://doi.org/10.1111/cge.12259.
54. Hu, Y., Flockhart, I., Vinayagam, A., Bergwitz, C., Berger, B., Perrimon, N., and Mohr, S.E. (2011). An integrative approach to ortholog prediction for disease-focused and other functional studies. BMC Bioinf. *12*, 357. https://doi.org/10.1186/1471-2105-12-357.
55. Diao, F., Ironfield, H., Luan, H., Diao, F., Shropshire, W.C., Ewer, J., Marr, E., Potter, C.J., Landgraf, M., and White, B.H. (2015). Plug-and-play genetic access to drosophila cell types using exchangeable exon cassettes. Cell Rep. *10*, 1410–1421. https://doi.org/10.1016/j.celrep.2015.01.059.
56. Nagarkar-Jaiswal, S., Lee, P.T., Campbell, M.E., Chen, K., Anguiano-Zarate, S., Gutierrez, M.C., Busby, T., Lin, W.W., He, Y., Schulze, K.L., et al. (2015). A library of MiMICs allows tagging of genes and reversible, spatial and temporal knockdown of proteins in Drosophila. Elife *4*, e05338. https://doi.org/10.7554/eLife.05338.
57. Lee, P.T., Zirin, J., Kanca, O., Lin, W.W., Schulze, K.L., Li-Kroeger, D., Tao, R., Devereaux, C., Hu, Y., Chung, V., et al. (2018). A gene-specific T2A-GAL4 library for Drosophila. Elife *7*, e35574. https://doi.org/10.7554/eLife.35574.
58. Golic, M.M., Rong, Y.S., Petersen, R.B., Lindquist, S.L., and Golic, K.G. (1997). FLP-mediated DNA mobilization to specific target sites in Drosophila chromosomes. Nucleic Acids Res. *25*, 3665–3671. https://doi.org/10.1093/nar/25.18.3665.
59. Yamamoto, S., Jaiswal, M., Charng, W.L., Gambin, T., Karaca, E., Mirzaa, G., Wiszniewski, W., Sandoval, H., Haelterman, N.A., Xiong, B., et al. (2014). A drosophila genetic resource of mutants to study mechanisms underlying human genetic diseases. Cell *159*, 200–214. https://doi.org/10.1016/j.cell.2014.09.002.
60. GTEx Consortium (2013). The Genotype-Tissue Expression (GTEx) project. Nat. Genet. *45*, 580–585. https://doi.org/10.1038/ng.2653.
61. Li, H., Janssens, J., De Waegeneer, M., Kolluru, S.S., Davie, K., Gardeux, V., Saelens, W., David, F.P.A., Brbić, M., Spanier, K., et al. (2022). Fly Cell Atlas: A single-nucleus transcriptomic atlas of the adult fruit fly. Science *375*, eabk2432. https://doi.org/10.1126/science.abk2432.
62. Ravenscroft, T.A., Janssens, J., Lee, P.T., Tepe, B., Marcogliese, P.C., Makhzami, S., Holmes, T.C., Aerts, S., and Bellen, H.J. (2020). Drosophila Voltage-Gated Sodium Channels Are Only Expressed in Active Neurons and Are Localized to Distal Axonal Initial Segment-like Domains. J. Neurosci. *40*, 7999–8024. https://doi.org/10.1523/JNEUROSCI.0142-20.2020.
63. Anzalone, A.V., Randolph, P.B., Davis, J.R., Sousa, A.A., Koblan, L.W., Levy, J.M., Chen, P.J., Wilson, C., Newby, G.A., Raguram, A., and Liu, D.R. (2019). Search-and-replace genome editing without double-strand breaks or donor DNA. Nature *576*, 149–157. https://doi.org/10.1038/s41586-019-1711-4.
64. Dolph, P., Nair, A., and Raghu, P. (2011). Electroretinogram recordings of Drosophila. Cold Spring Harb. Protoc. *2011*, pdb.prot5549. pdb prot5549. https://doi.org/10.1101/pdb.prot5549.
65. Kanca, O., Zirin, J., Garcia-Marques, J., Knight, S.M., Yang-Zhou, D., Amador, G., Chung, H., Zuo, Z., Ma, L., He, Y., et al. (2019). An efficient CRISPR-based strategy to insert small and large fragments of DNA using short homology arms. Elife *8*, e51539. https://doi.org/10.7554/eLife.51539.
66. Kanca, O., Zirin, J., Hu, Y., Tepe, B., Dutta, D., Lin, W.W., Ma, L., Ge, M., Zuo, Z., Liu, L.P., et al. (2022). An expanded toolkit for Drosophila gene tagging using synthesized homology donor constructs for CRISPR-mediated homologous recombination. Elife *11*, e76077. https://doi.org/10.7554/eLife.76077.
67. Yamamoto, S., Kanca, O., Wangler, M.F., and Bellen, H.J. (2024). Integrating non-mammalian model organisms in the diagnosis of rare genetic diseases in humans. Nat. Rev. Genet. *25*, 46–60. https://doi.org/10.1038/s41576-023-00633-6.
68. Chavali, V.R.M., Khan, N.W., Cukras, C.A., Bartsch, D.U., Jablonski, M.M., and Ayyagari, R. (2011). A CTRP5 gene S163R mutation knock-in mouse model for late-onset retinal degeneration. Hum. Mol. Genet. *20*, 2000–2014. https://doi.org/10.1093/hmg/ddr080.
69. Şahin, A., Held, A., Bredvik, K., Major, P., Achilli, T.M., Kerson, A.G., Wharton, K., Stilwell, G., and Reenan, R. (2017). Human SOD1 ALS Mutations in a Drosophila Knock-In Model Cause Severe Phenotypes and Reveal Dosage-Sensitive Gain- and Loss-of-Function Components. Genetics *205*, 707–723. https://doi.org/10.1534/genetics.116.190850.
70. Sun, L., Gilligan, J., Staber, C., Schutte, R.J., Nguyen, V., O'Dowd, D.K., and Reenan, R. (2012). A knock-in model of human epilepsy in Drosophila reveals a novel cellular mechanism associated with heat-induced seizure. J. Neurosci. *32*, 14145–14155. https://doi.org/10.1523/JNEUROSCI.2932-12.2012.
71. Yin, H.Z., Nalbandian, A., Hsu, C.I., Li, S., Llewellyn, K.J., Mozaffar, T., Kimonis, V.E., and Weiss, J.H. (2012). Slow development of ALS-like spinal cord pathology in mutant valosin-containing protein gene knock-in mice. Cell Death Dis. *3*, e374. https://doi.org/10.1038/cddis.2012.115.
72. Li-Kroeger, D., Kanca, O., Lee, P.T., Cowan, S., Lee, M.T., Jaiswal, M., Salazar, J.L., He, Y., Zuo, Z., and Bellen, H.J. (2018). An expanded toolkit for gene tagging based on MiMIC and scarless CRISPR tagging in Drosophila. Elife *7*, e38709. https://doi.org/10.7554/eLife.38709.
73. Rios, J.J., Denton, K., Russell, J., Kozlitina, J., Ferreira, C.R., Lewanda, A.F., Mayfield, J.E., Moresco, E., Ludwig, S., Tang, M., et al. (2021). Germline Saturation Mutagenesis Induces Skeletal Phenotypes in Mice. J. Bone Miner. Res. *36*, 1548–1565. https://doi.org/10.1002/jbmr.4323.
74. Cornils, H., Stegert, M.R., Hergovich, A., Hynx, D., Schmitz, D., Dirnhofer, S., and Hemmings, B.A. (2010). Ablation of the kinase NDR1 predisposes mice to the development of T cell lymphoma. Sci. Signal. *3*, ra47. https://doi.org/10.1126/scisignal.2000681.
75. Rehberg, K., Kliche, S., Madencioglu, D.A., Thiere, M., Müller, B., Meineke, B.M., Freund, C., Budinger, E., and Stork, O. (2014). The serine/threonine kinase Ndr2 controls integrin trafficking and integrin-dependent neurite growth. J. Neurosci. *34*, 5342–5354. https://doi.org/10.1523/JNEUROSCI.2728-13.2014.
76. Léger, H., Santana, E., Leu, N.A., Smith, E.T., Beltran, W.A., Aguirre, G.D., and Luca, F.C. (2018). Ndr kinases regulate retinal interneuron proliferation and homeostasis. Sci. Rep. *8*, 12544. https://doi.org/10.1038/s41598-018-30492-9.